



Earth Observation and Environmental Remote Sensing Laboratory
Abu Dhabi, United Arab Emirates
[hghedira @masdar.ac.ae](mailto:hghedira@masdar.ac.ae)

Early Adopter Presentation:
**Estimating and Mapping the Extent of Saharan Dust Emissions
Using SMAP-derived soil moisture data**

Hosni Ghedira – Imen Gherboudj –Naseema S Beegum-Sagar Prasad Parajuli

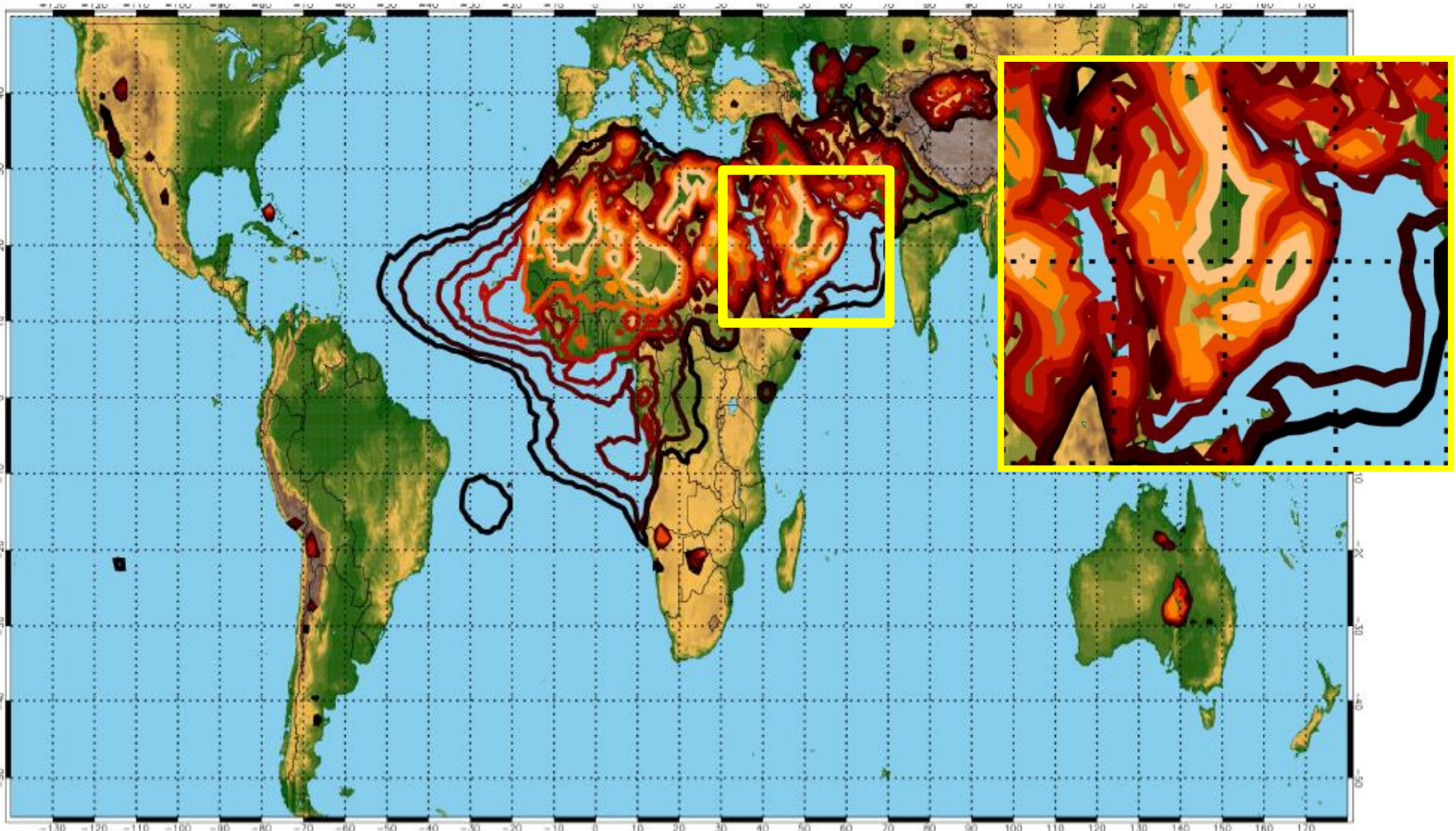
2nd Soil Moisture Active Passive (SMAP) Applications Workshop
USDA South Building
Washington DC
October 12-13 2011

Objective

→ To explore the potential of SMAP-derived soil moisture to improve existing dust detection tools in desert and arid environment.

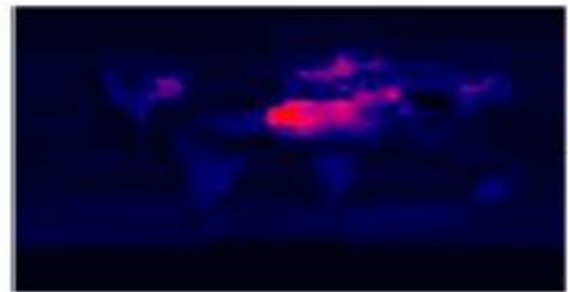
- 🌀 Anomalies in dust generation are closely related to water content in the upper soil layer which has a direct effect on the availability of loose sediments.
- 🌀 In addition to wind speed and direction, other land features such as vegetation cover and soil type would also affect the dynamic of dust generation.

*Frequency of Occurrence TOMS Aerosol Index (Version 7) greater than 0.5 per year
averaged from 1980 to 1992.*

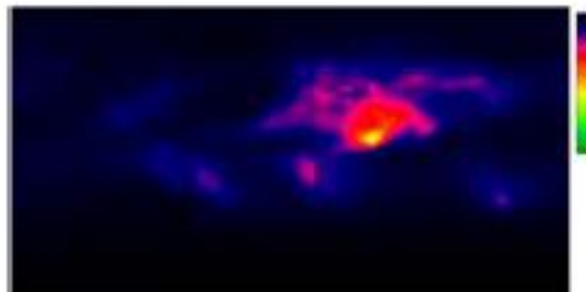


Source: Paul Ginoux, NOAA Geophysical Fluid Dynamics Laboratory, Princeton, NJ

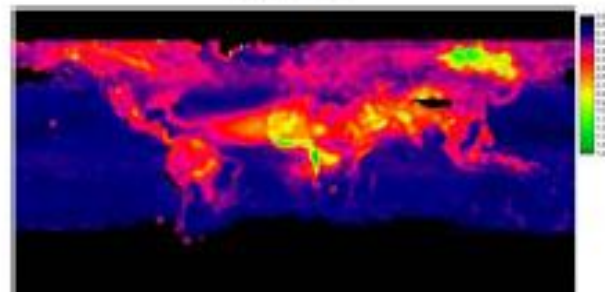
Uncertainty in Aerosol Retrieval



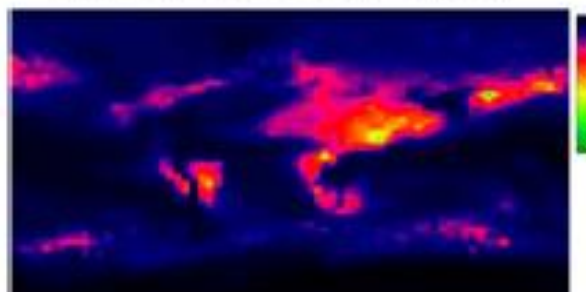
GADS



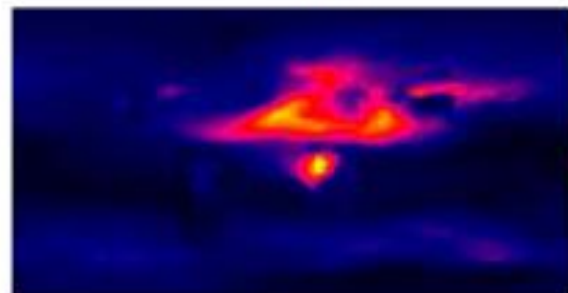
NASA GISS v1 / GACP



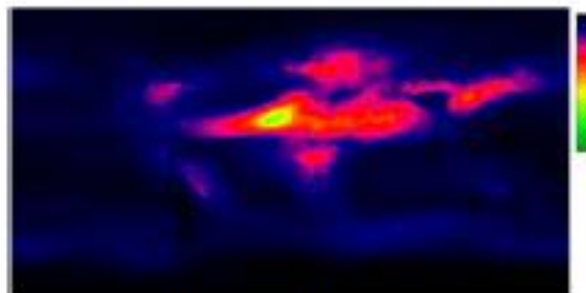
Toms



NASA GISS v2 1990

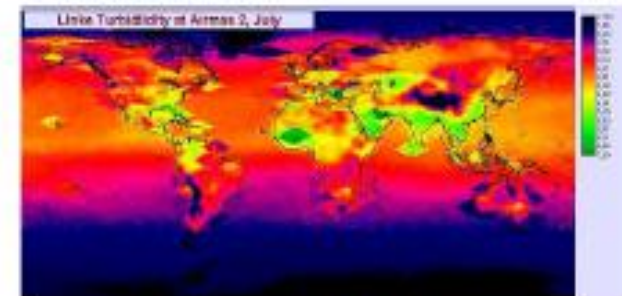


GOCART



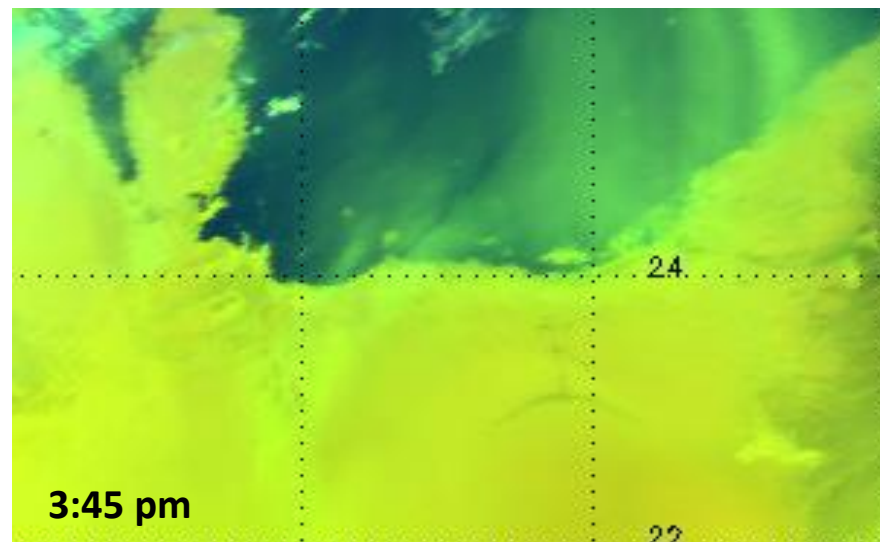
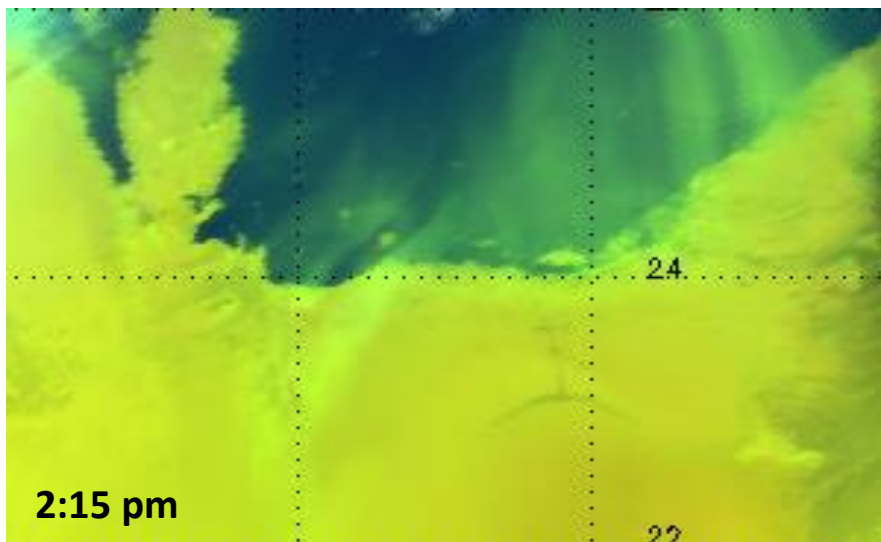
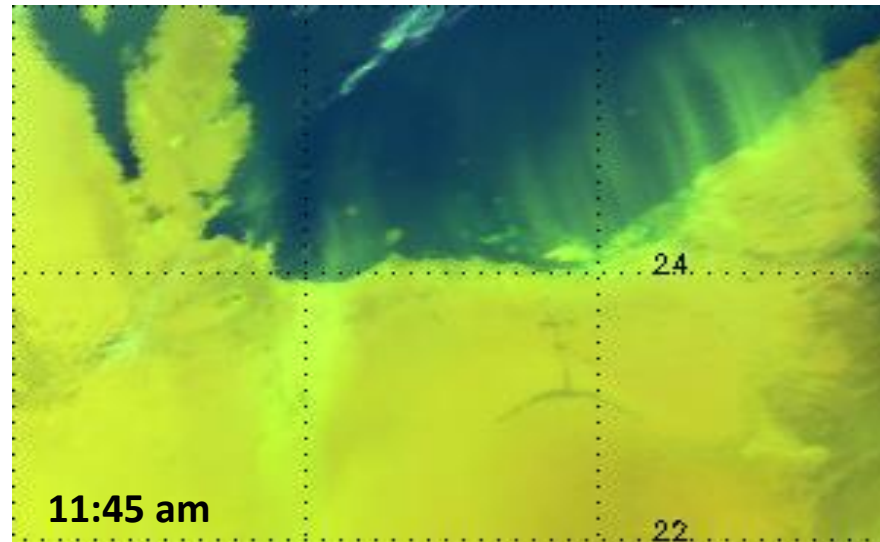
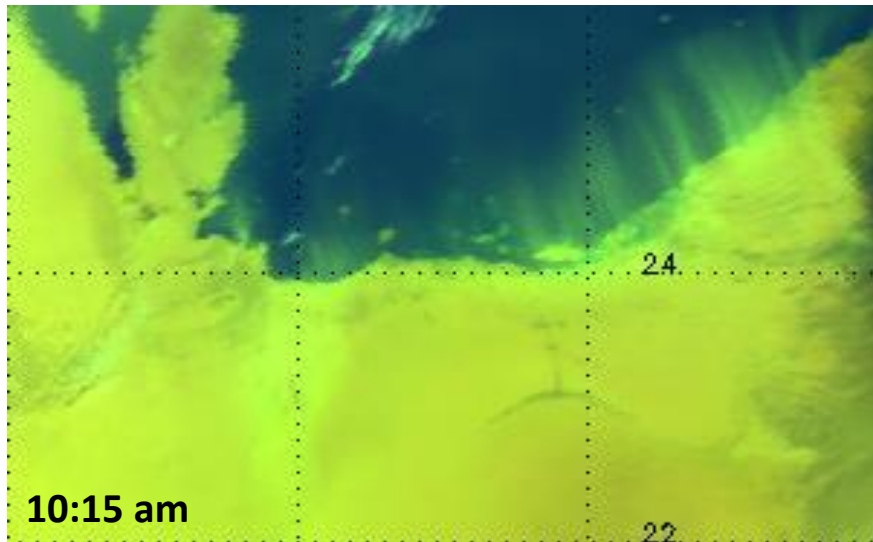
AeroCom

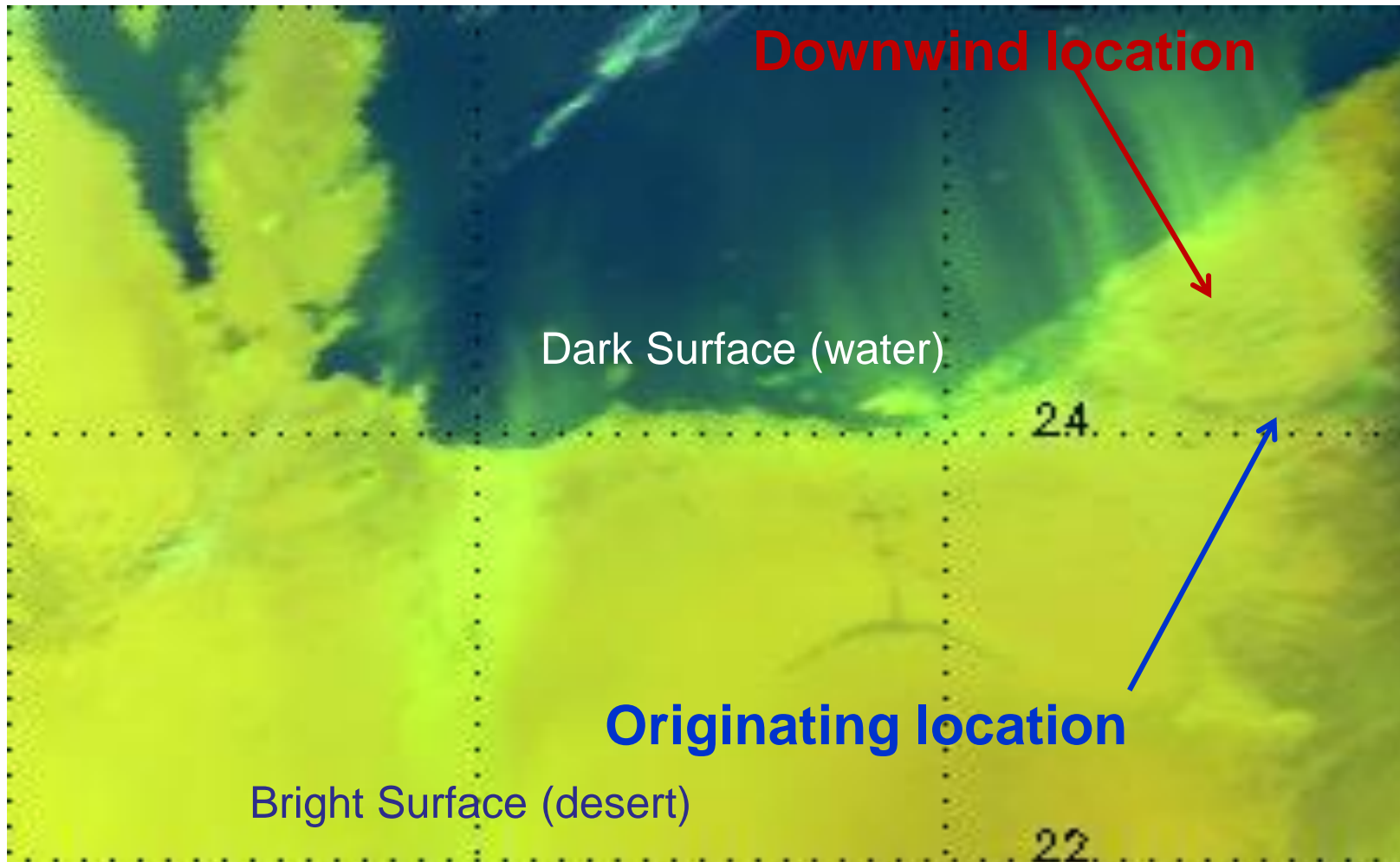
- All graphs are for July
- Scales are the same! (0 – 1.5)
- Large differences in Aerosol values and distribution



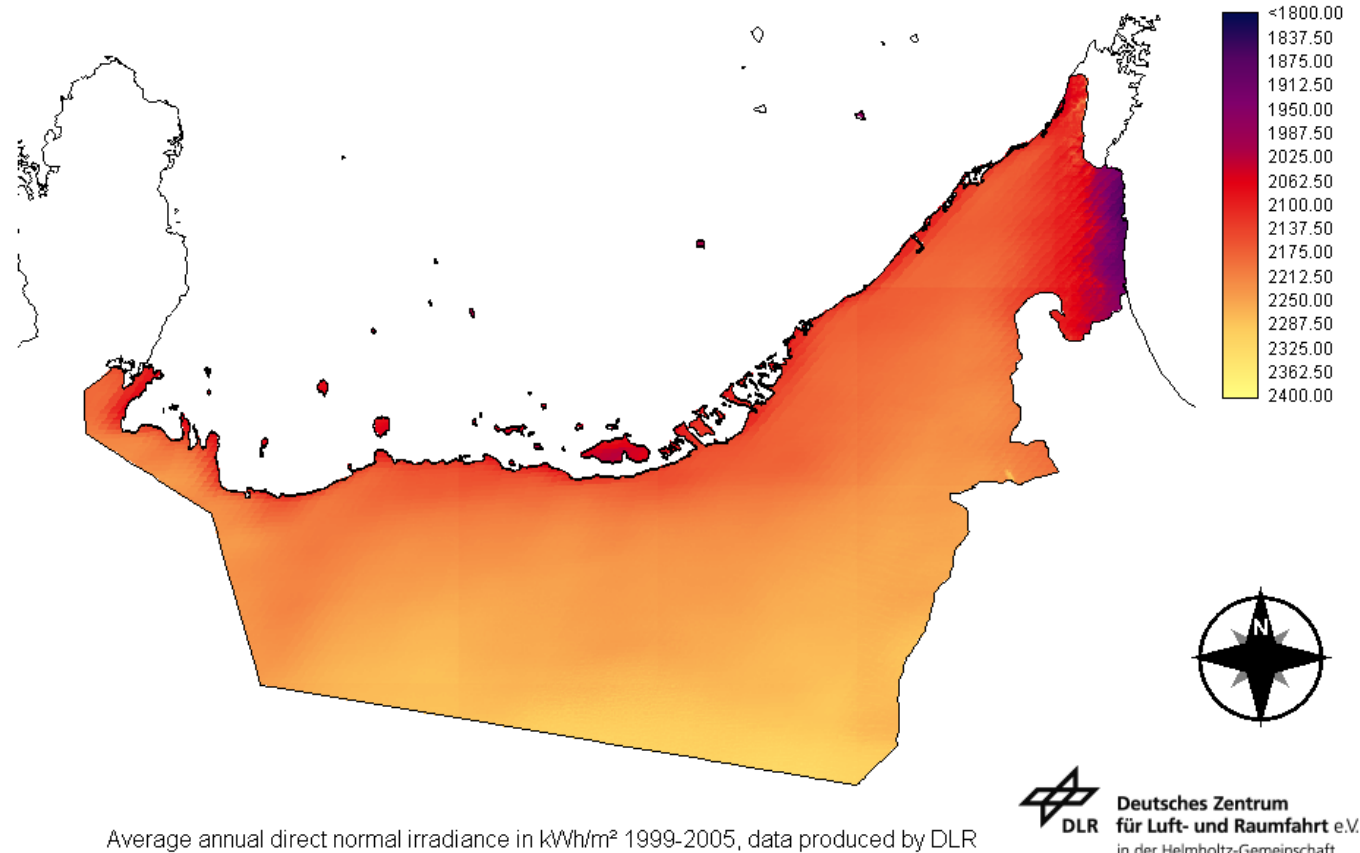
Linke Turbidity

Dust storm event over the UAE captured by METEOSAT-SEVIRI on February 12, 2009





Assessing Solar Energy Potential in Arid and Desert Environment: the UAE Case Study



Average annual direct normal irradiance in kWh/m² 1999-2005, data produced by DLR

~ 95%

Energy-Generating Performance (%)

~ 60%

~150

Suspended Dust Concentration (ppm)

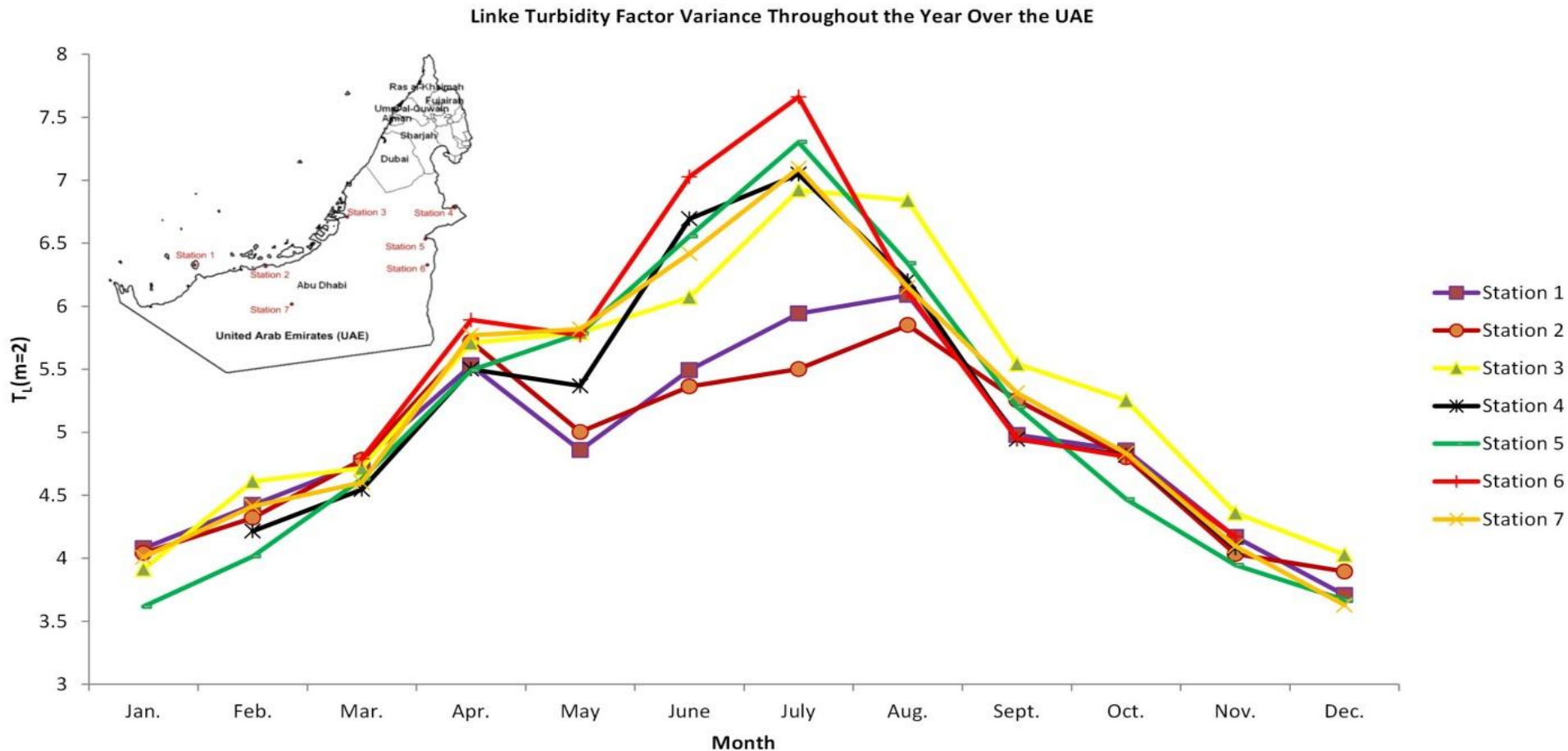
~2500



Deutsches Zentrum
für Luft- und Raumfahrt e.V.
in der Helmholtz-Gemeinschaft

Energy-generating of PV modules can be reduced by as much as 40 % in dusty weather.

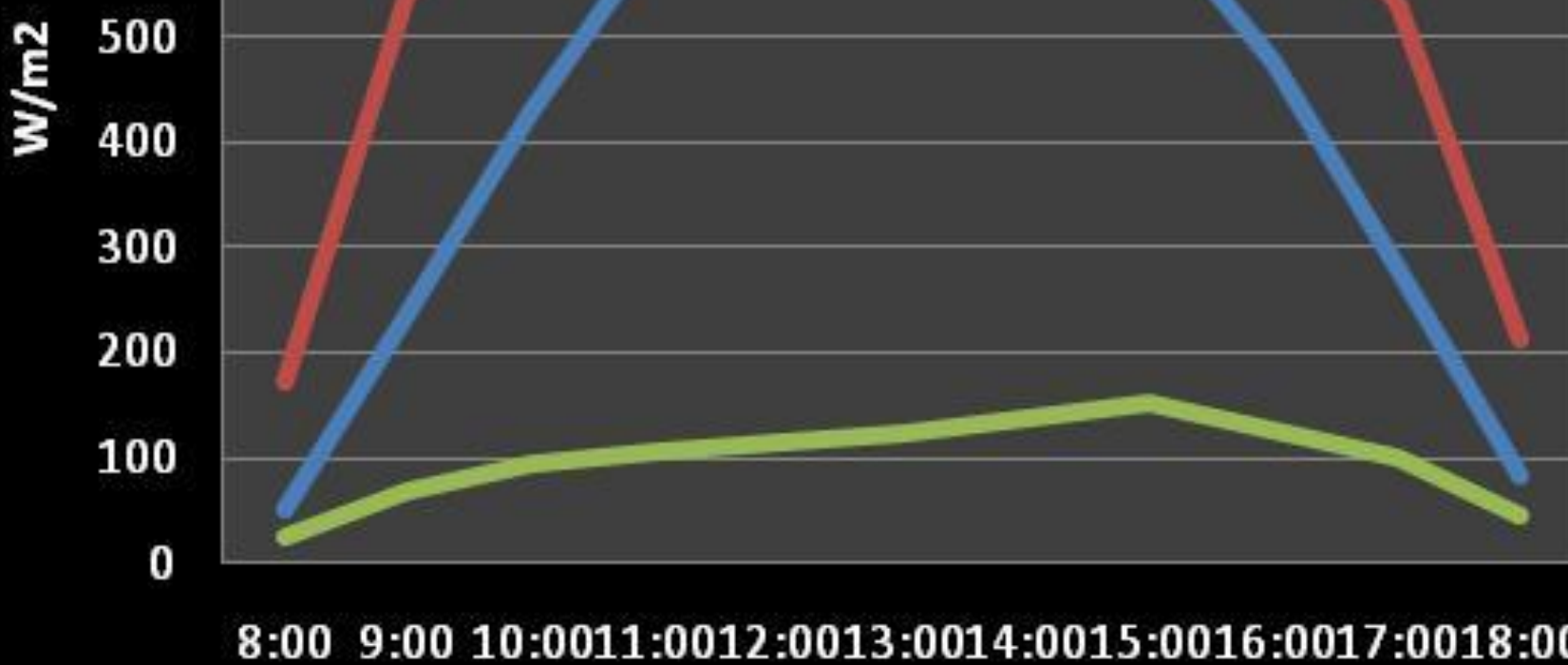
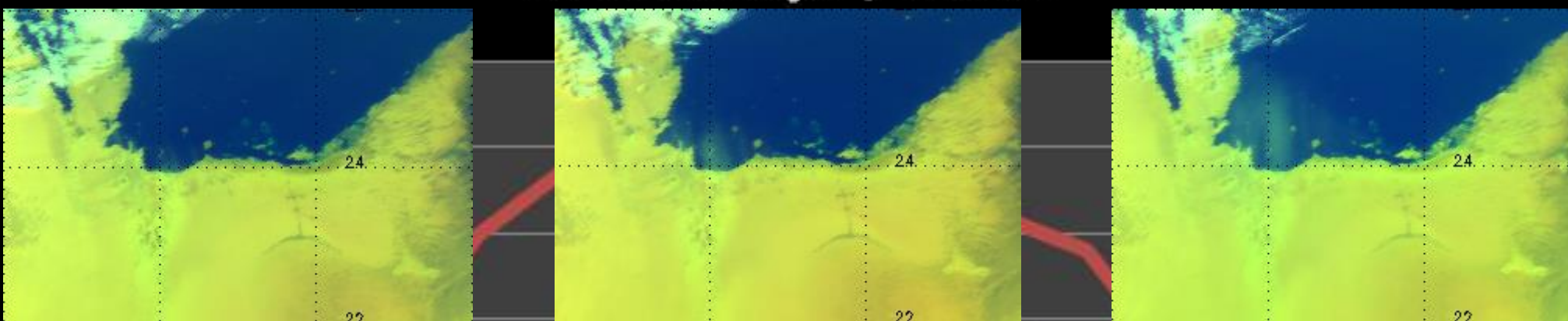
Temporal and Spatial Variability of Atmospheric Turbidity in the UAE



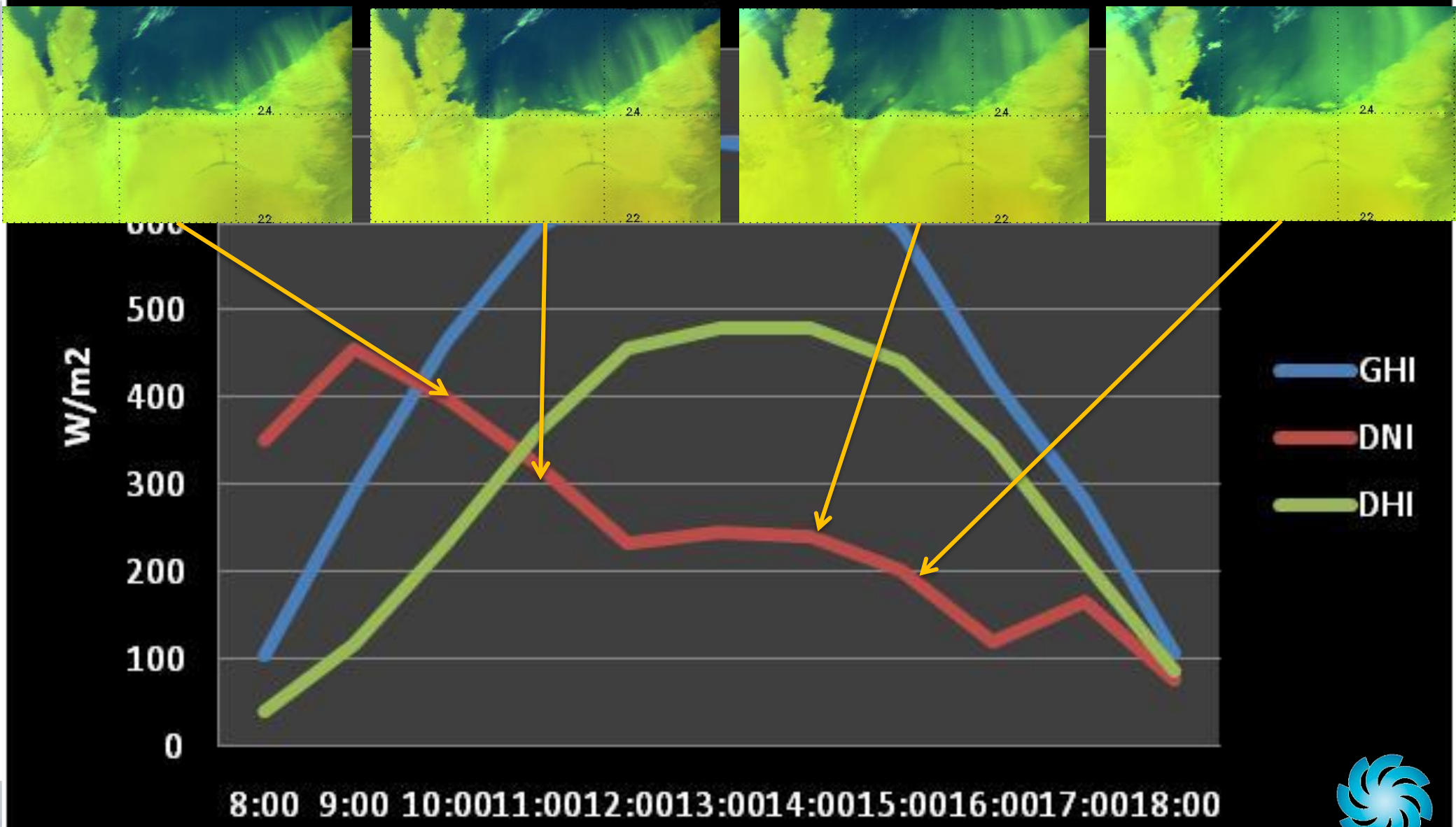
Eissa, Ghedira and Chiesa (2011)

Clear Day

February 1, 2009

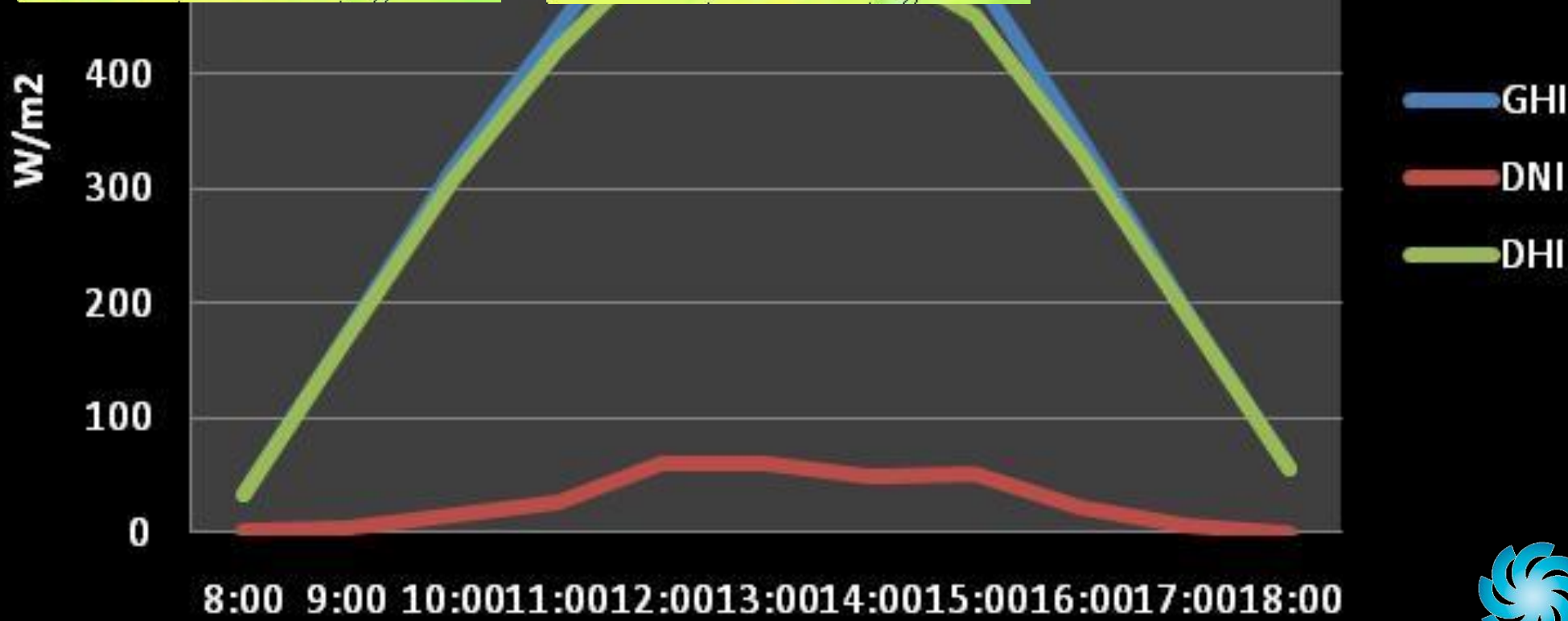
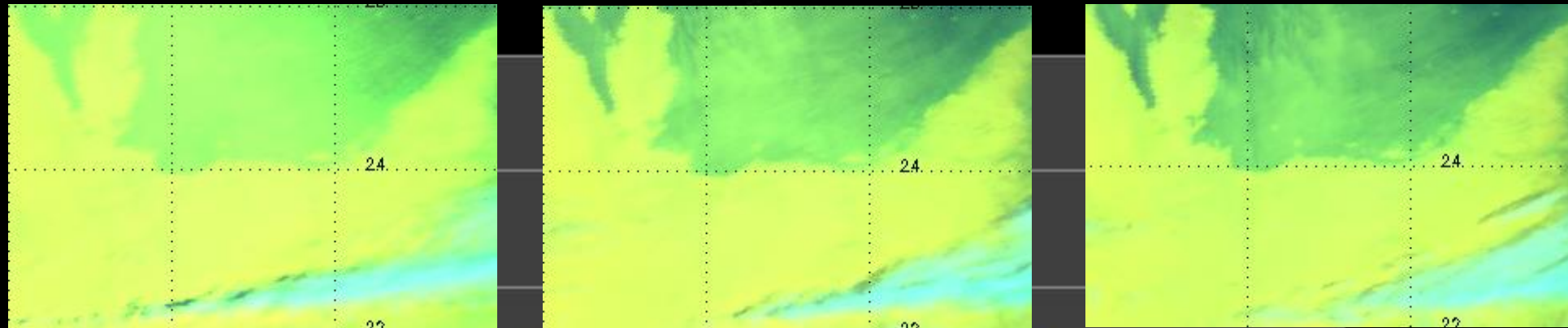


Moderate Dust February 28, 2009

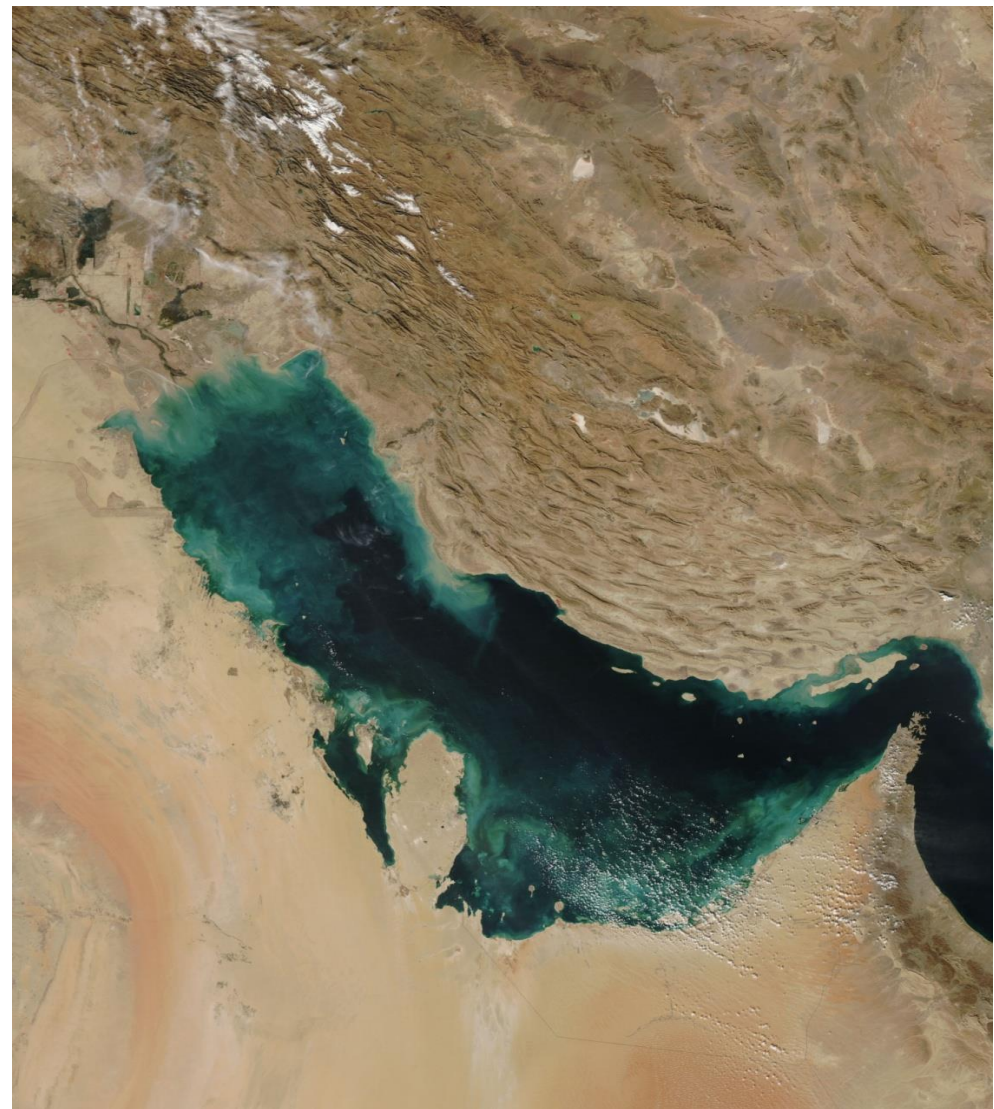
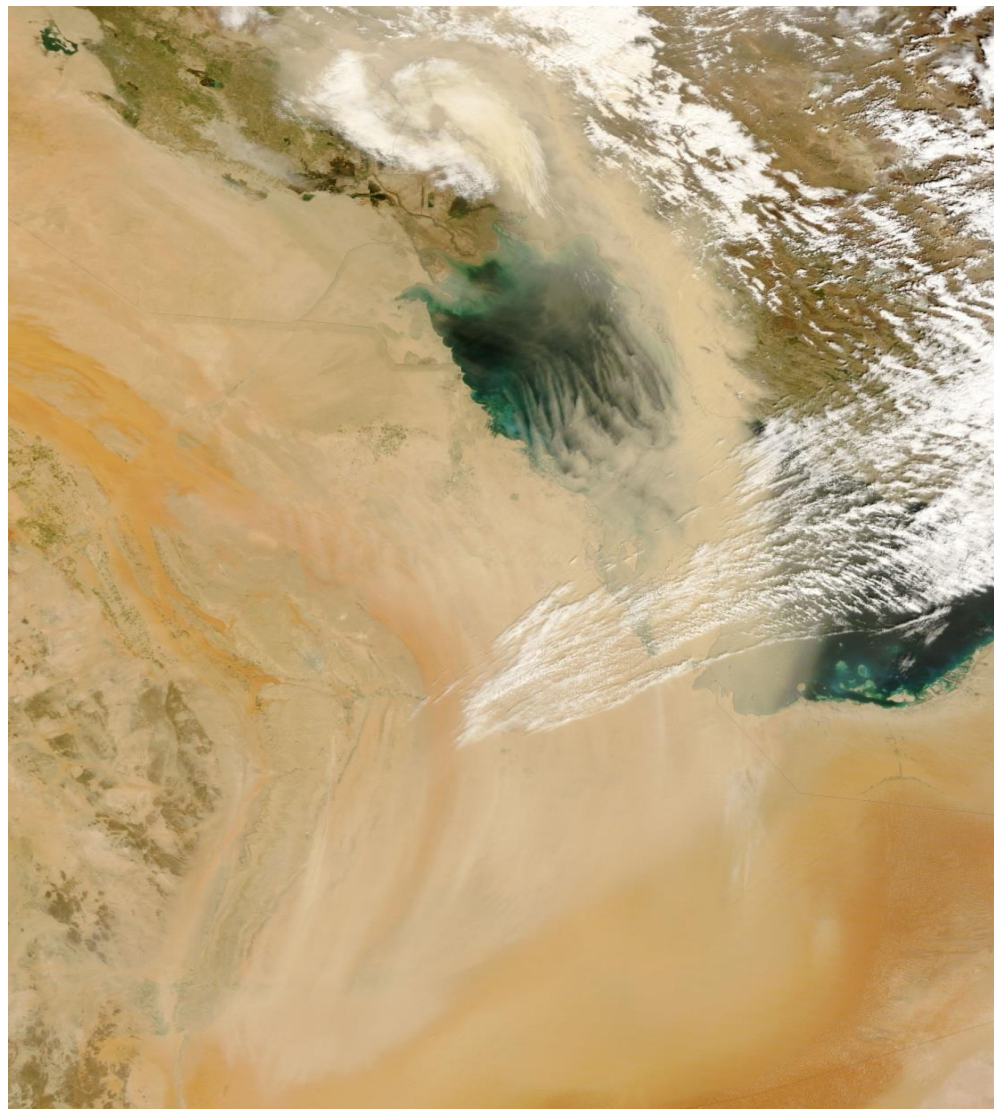


Heavy Dust

February 12, 2009



MODIS Data



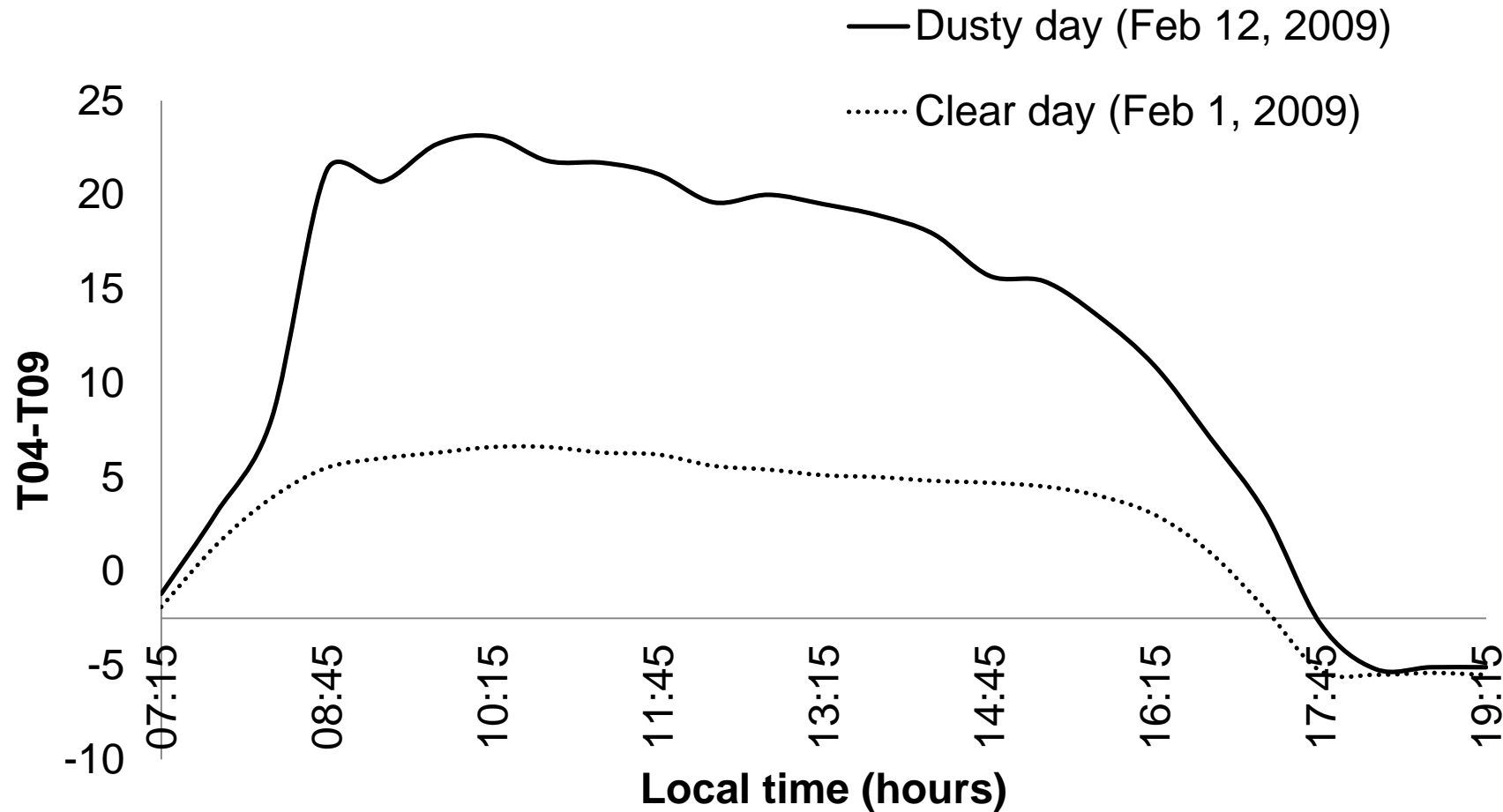
Dust detection using thermal channels

- ✿ $\text{BT}_{11}-\text{BT}_{12}$ is negative in the presence of dust²
- ✿ $\text{BT}_{8.5}-\text{BT}_{11}$ varies from positive to negative depending upon the concentration of dust²
- ✿ $\text{BT}_{11}-\text{BT}_{12}$ generally positive for clouds and negative for dust¹
- ✿ Both difference increase with the increase in aerosol optical thickness, AOT¹

(¹ Ackerman, 1997)

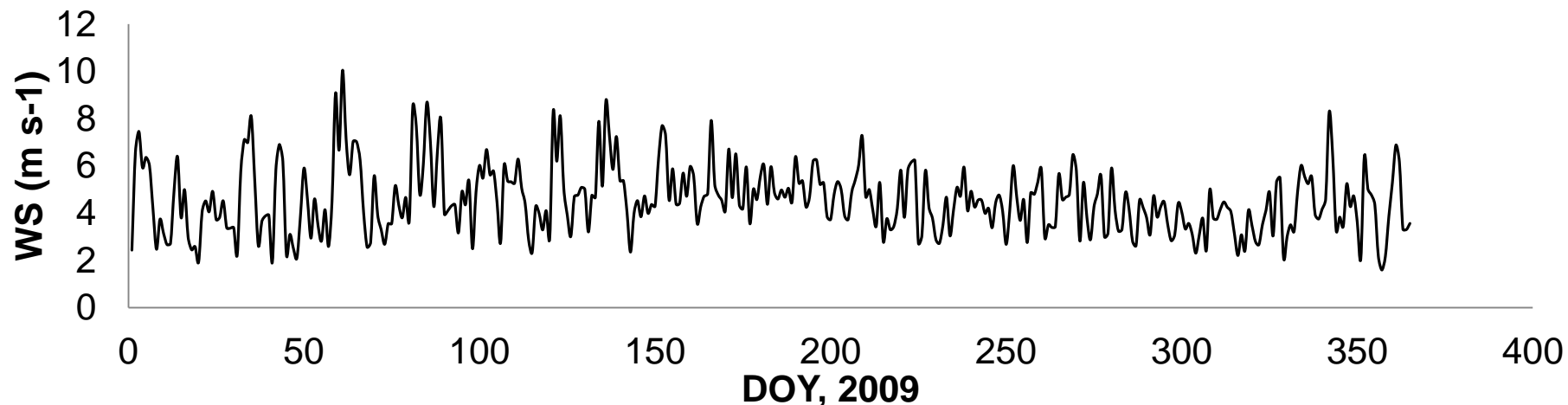
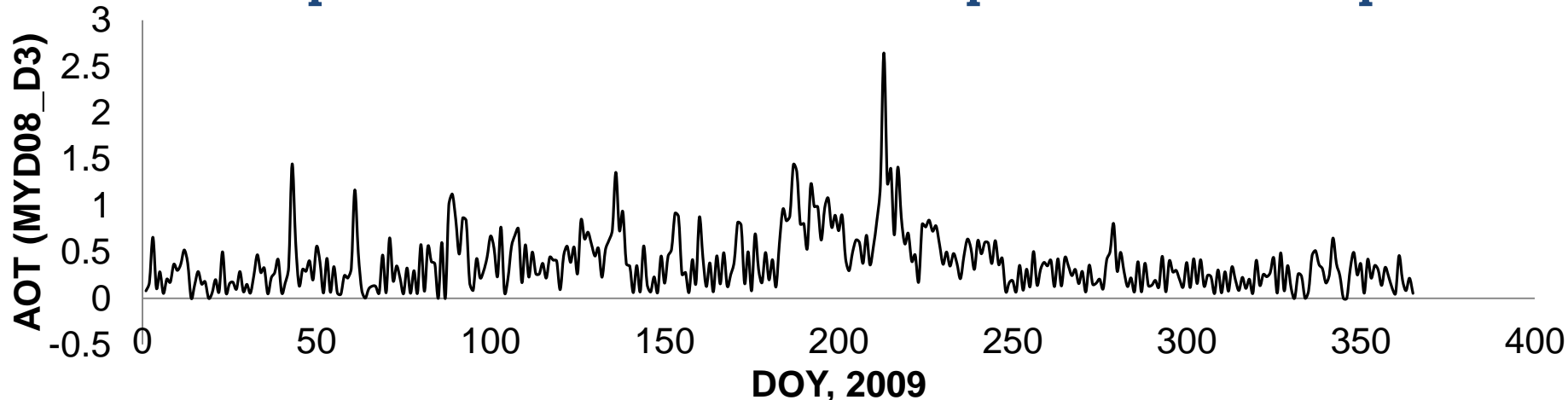
(² Zhang, Lu, Hu, & Dong, 2006)

Daily variation of T04-T09



Aerosol optical depth

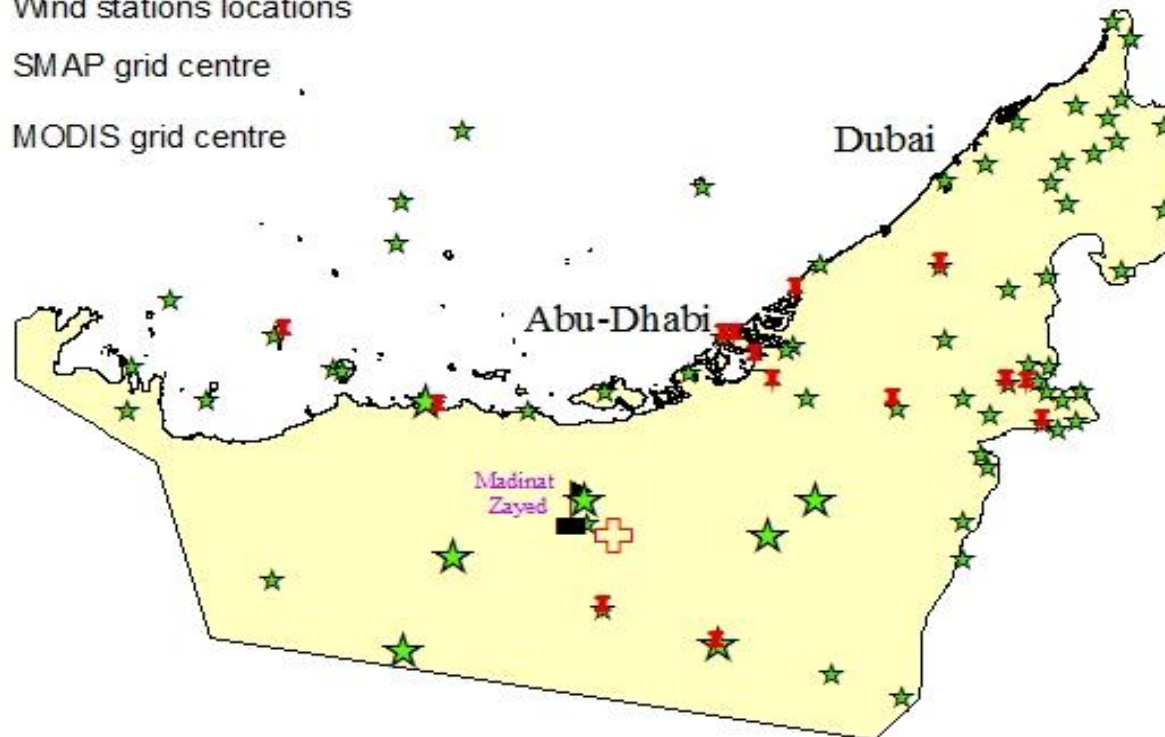
Temporal variation of MODIS Deep blue and wind speed



Study site

United Arab Emirates

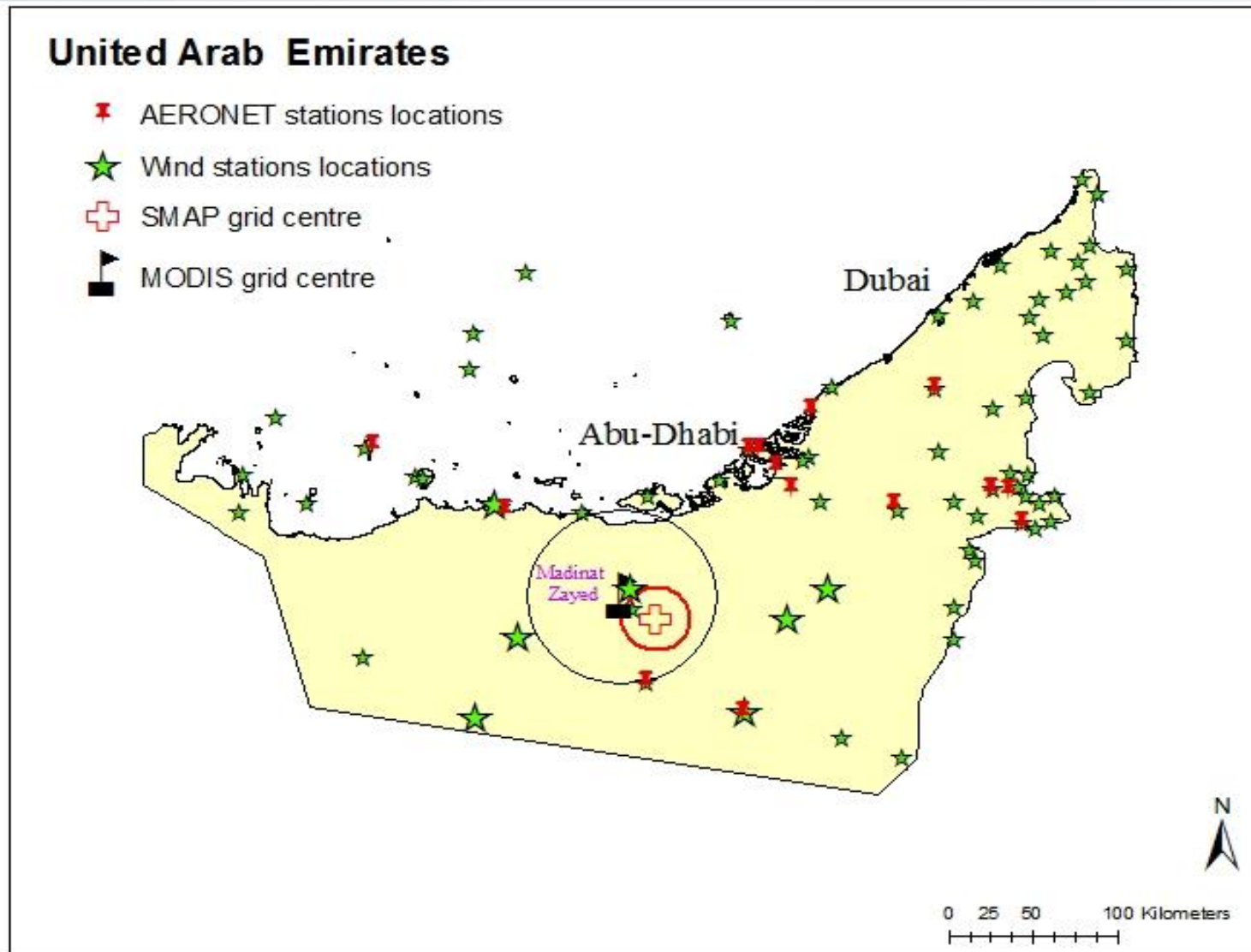
- ✖ AERONET stations locations
- ★ Wind stations locations
- ✚ SMAP grid centre
- ⚑ MODIS grid centre



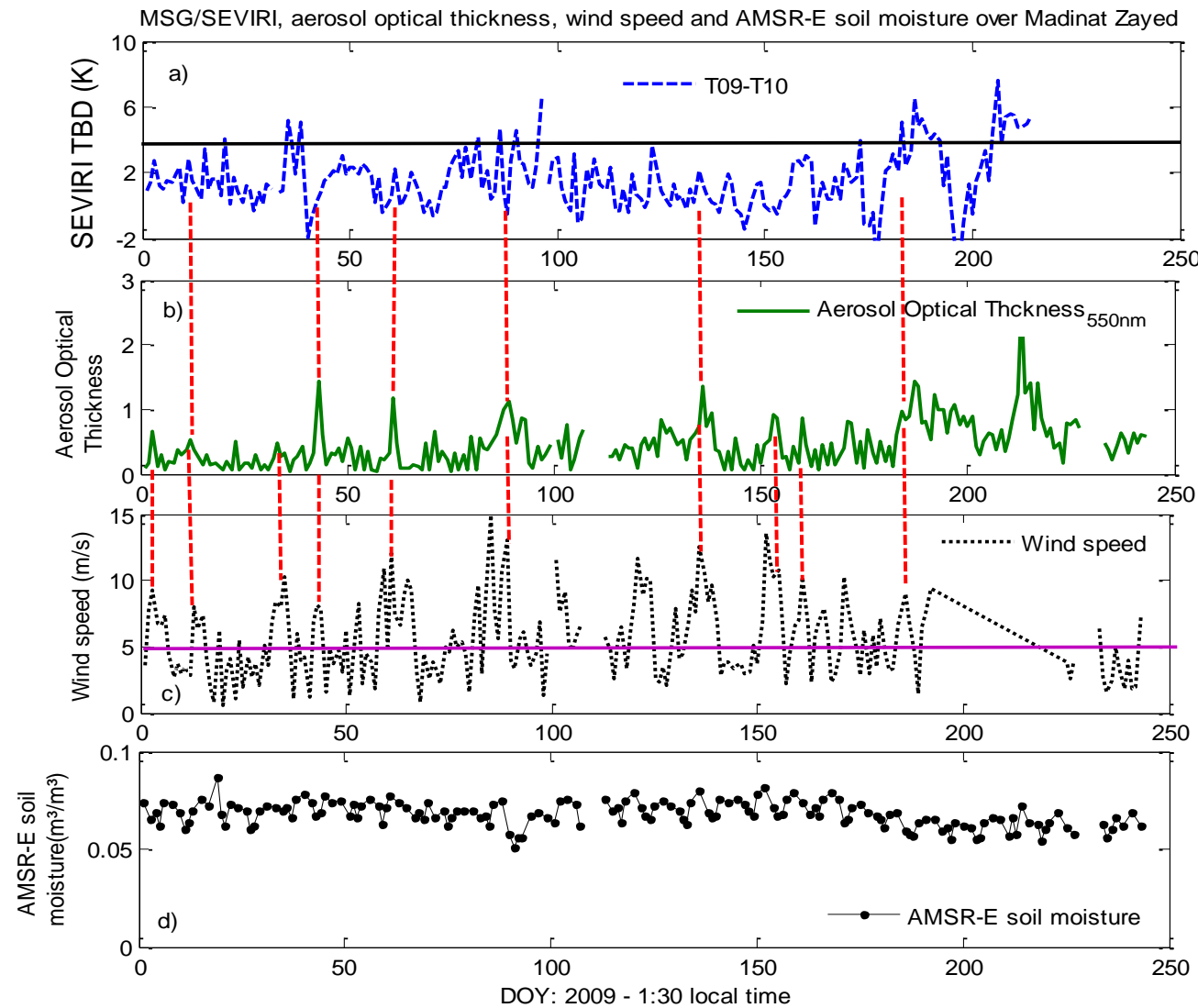
0 25 50 100 Kilometers

N

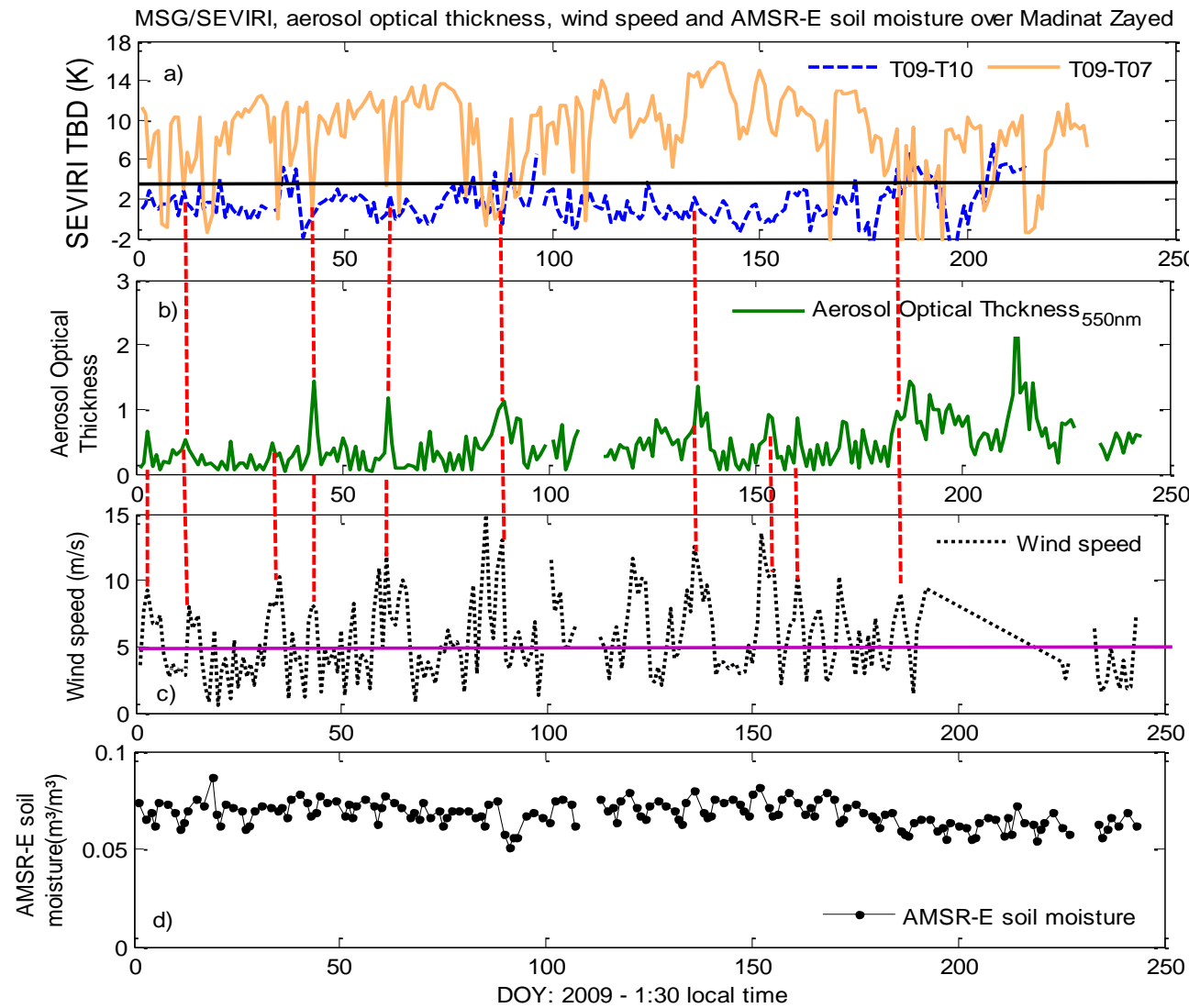
Study site



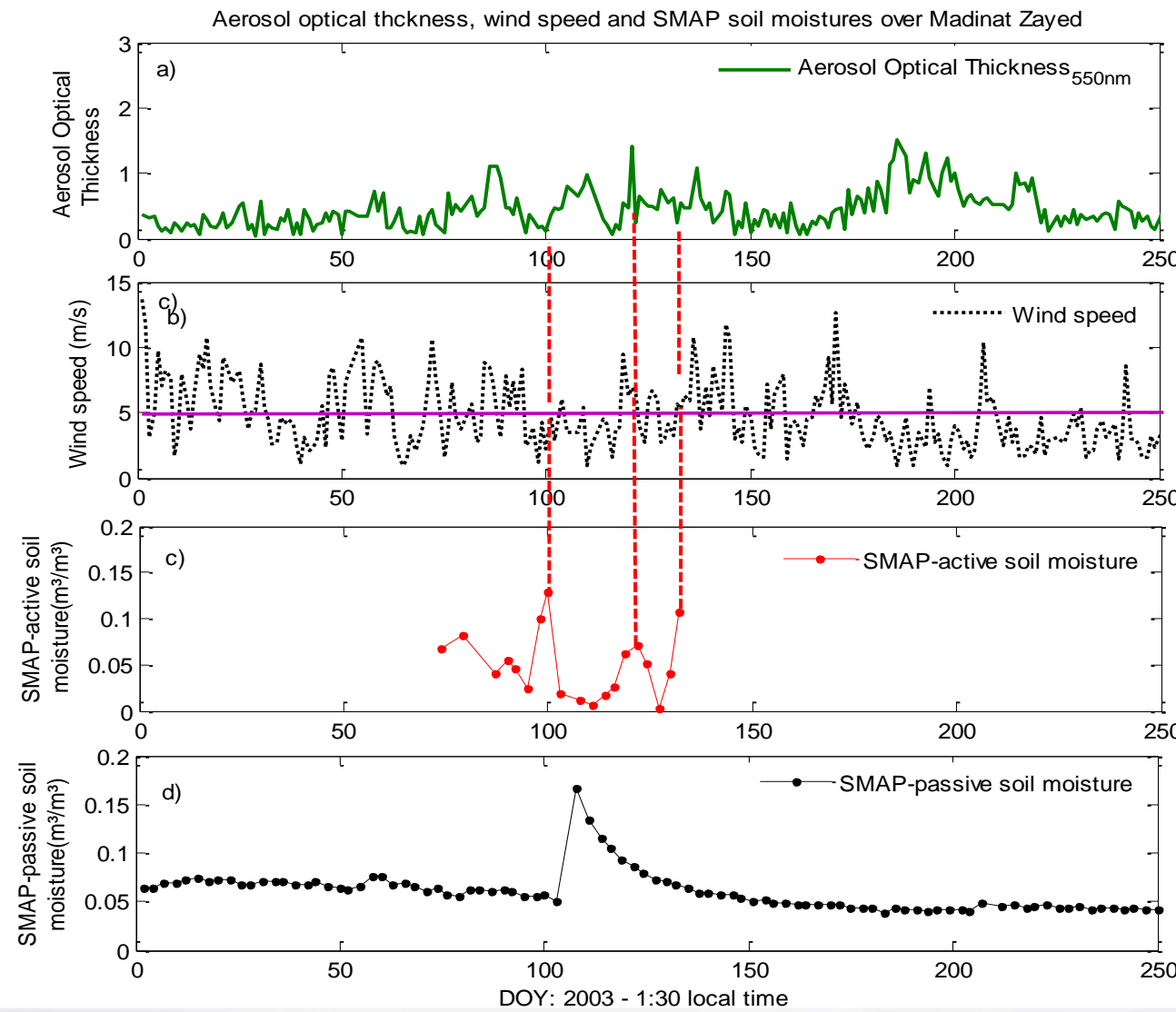
Temporal variation of Dust index, MODIS Deep blue, wind speed, AMSR-E soil moisture



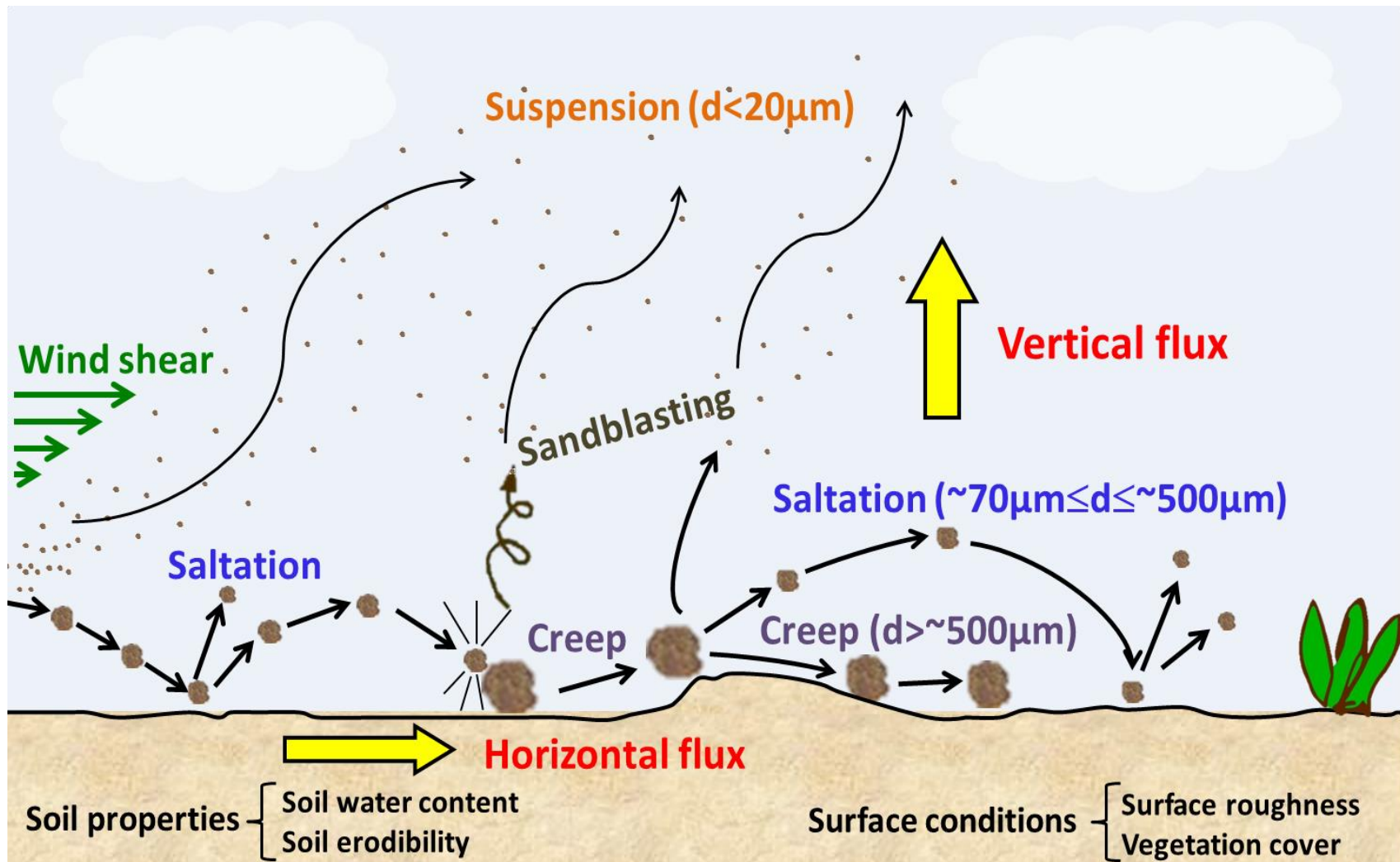
Temporal variation of Dust index, MODIS Deep blue, wind speed, AMSR-E soil moisture



Temporal variation of MODIS Deep blue, wind speed, SMAP soil moisture



Dust emission



Gherboudj et al., 2016

Alfaro and Gomes parameterization scheme for dust emission (2001)

1a. Friction velocity:

$$u_* = \frac{U_s(z)}{k} \ln\left(\frac{z}{z_0}\right)$$

1b. Threshold friction velocity for smooth surface:

$$u'_{ts} = \sqrt{a_n \left(\frac{\rho_p g D_s}{\rho_a} + \frac{\Gamma}{\rho_a D_s} \right)}$$

2. Corrected threshold friction velocity:

$$u_{*t} = f_w u'_{ts} / f_{eff}$$

$$f_{eff} = \left[1 - \left(\frac{\ln(z_0/z_{0s})}{\ln(0.35(10/z_{0s})^{0.8})} \right) \right]$$

$$f_w = \begin{cases} 1 & \text{for } w \leq w_t \\ \sqrt{1 + 1.21[w - w_t]^{0.68}} & \text{for } w > w_t \end{cases}$$

$$w_t = 0.17(\%_{clay}) + 0.0014(\%_{clay})^2$$

3a. **Horizontal flux:** $F_h = E(1-V)k \frac{\rho_a}{g} u_*^3 \left(1 + \frac{u_{*t}}{u_*} \right) \left(1 - \frac{u_{*t}^2}{u_*^2} \right) \int dS_{rel}(D_p) dD_p$

3b. **Vertical flux:** $F_{v,m,i}(D_p) = \sum_{k=1}^{N_{class}} \frac{\pi}{6} \frac{\rho_p \beta p_i(D_{p,k}) d_{m,i}^3}{e_i} dF_h(D_{p,k})$ (in $\mu\text{gm}^{-2}\text{s}^{-1}$)

Required parameters:

- a_n : constant (0.0123)
- Γ : constant (300 kgm^{-2})
- g : acceleration due to gravity
- D_s : soil particle size distribution (m)
- w_t : gravimetric soil moisture (%)
- z_0 : aeolian roughness length (m)
- z_{0s} : smooth roughness length ($D_{med}/30$)
- D_{med} : median diameter of coarsest mode (m)
- ρ_p : soil particle density (2650 kg m^{-3})
- ρ_a : air density (1.23 kgm^{-3})
- k : Von Karman constant (0.4)
- U_s : wind speed at height z (m/s)
- z_0 : surface roughness length (m)
- S_{rel} : relative surface area of each size bin
- e_i : cohesion energy
- d_m : log-normal modes (m=1, 2, 3)
- p_i : fraction of kinetic energy
- β : constant (163 ms^{-1})
- k : constant (1 for desert surfaces)
- E: erodibility factor of the soil
- V: fraction of vegetation.

Field operations for the Extensive Survey October 2006 - October 2007



a) Twin Ring Infiltrometer



c) Guelph Permeameter



b) Disk Permeameter



d) Penetrometer



Soil survey was performed using standards of the USDA Soil Survey Manual
(Soil Survey Division Staff, 1993; Schoeneberger *et al.* 2002)

More than **700 measurements** were undertaken at more than 70 sites.

Instruments used for measuring soil hydraulic properties and soil strength.

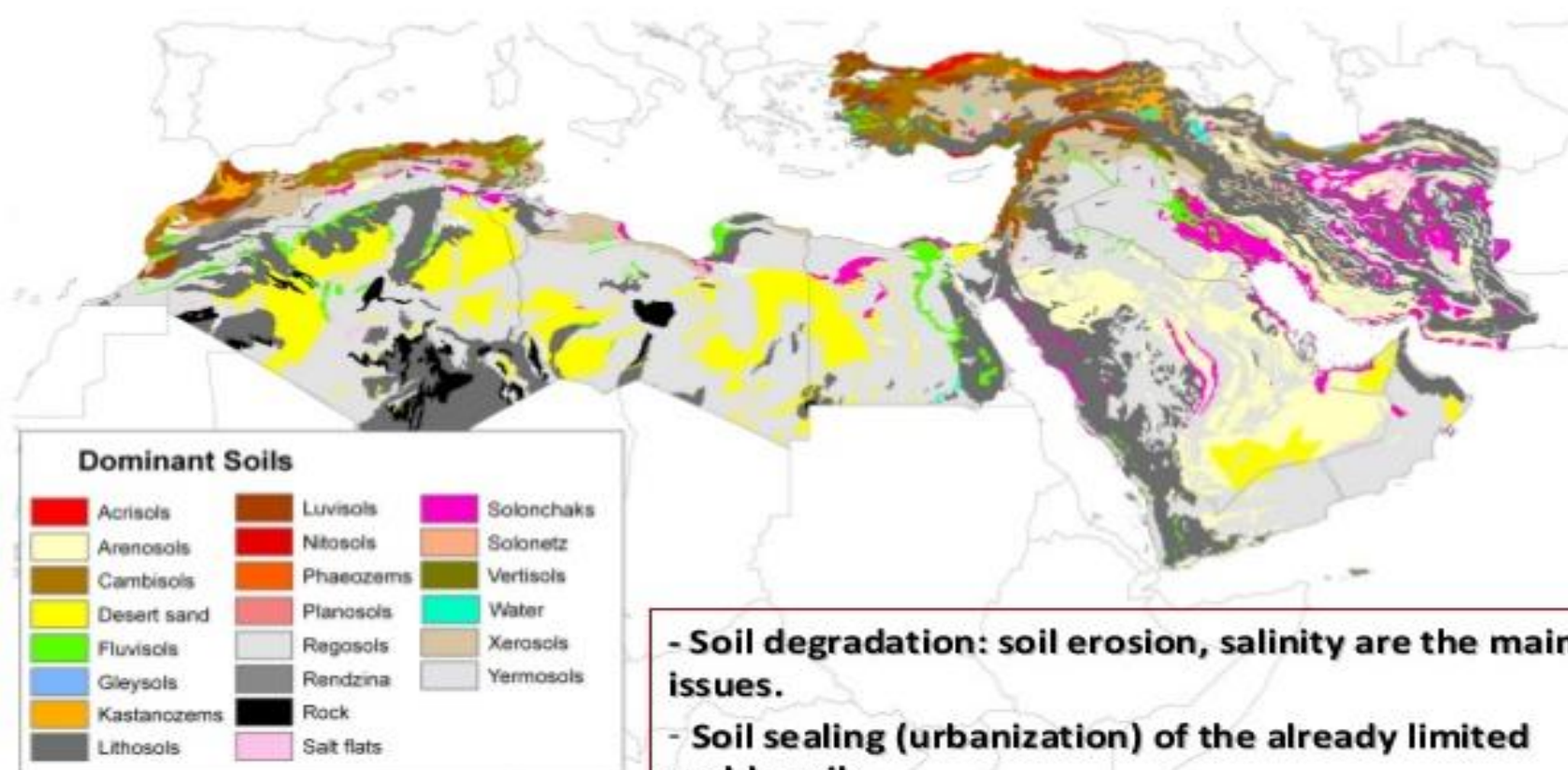


Study Area: Soil Types



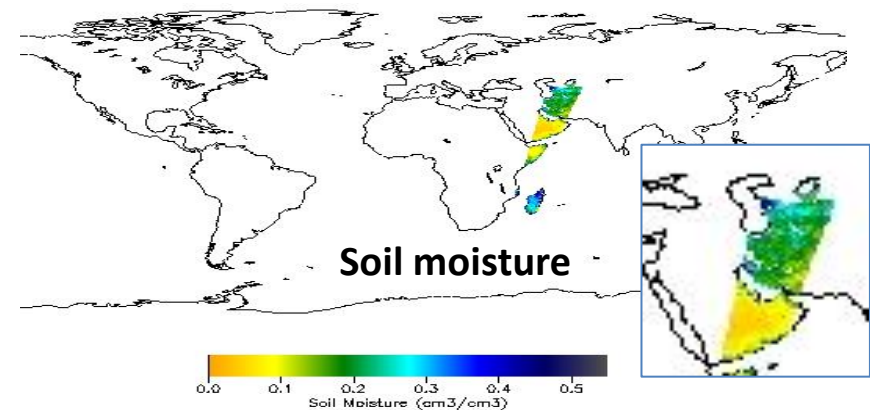
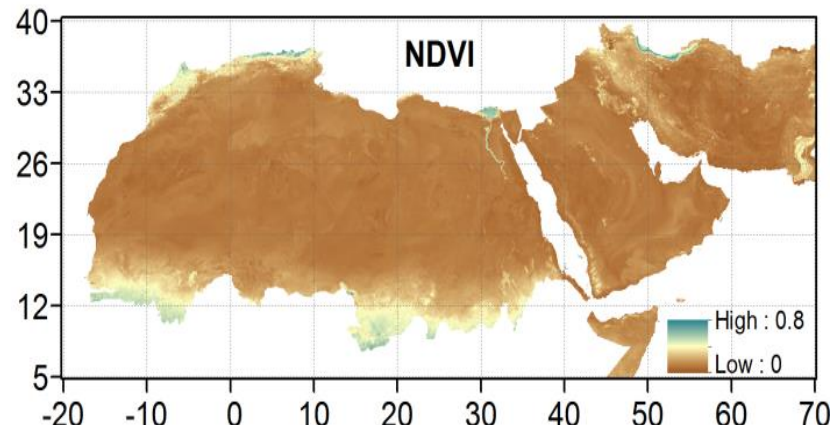
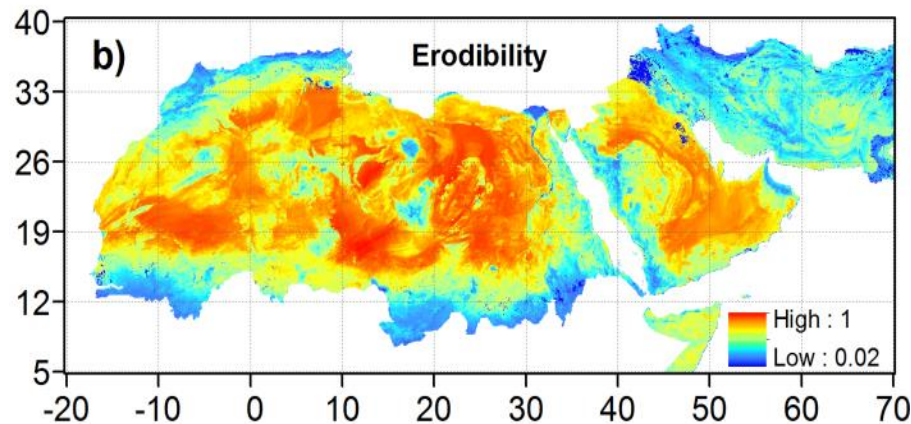
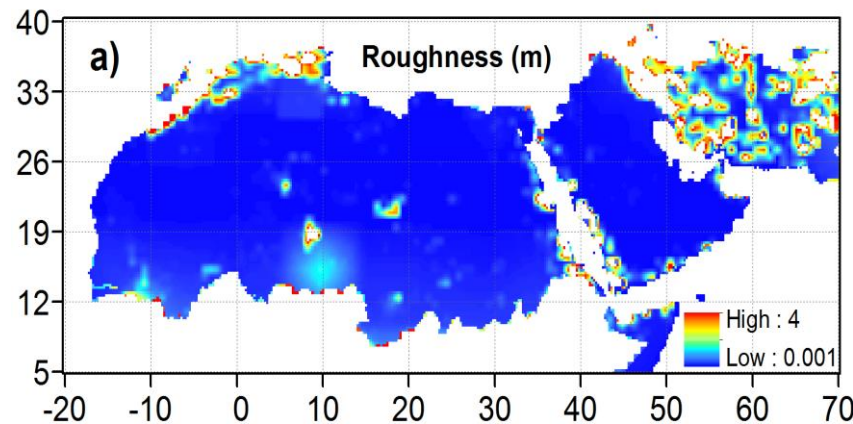
Plate 10: Typical landforms described during the field survey: a) saline sabkha plain; b) gypsum deflation plain; c) undulating sand sheet in the Madinat Zayed area; d) rolling dunes with Jabal Hafit in the background.

Soil Type Map



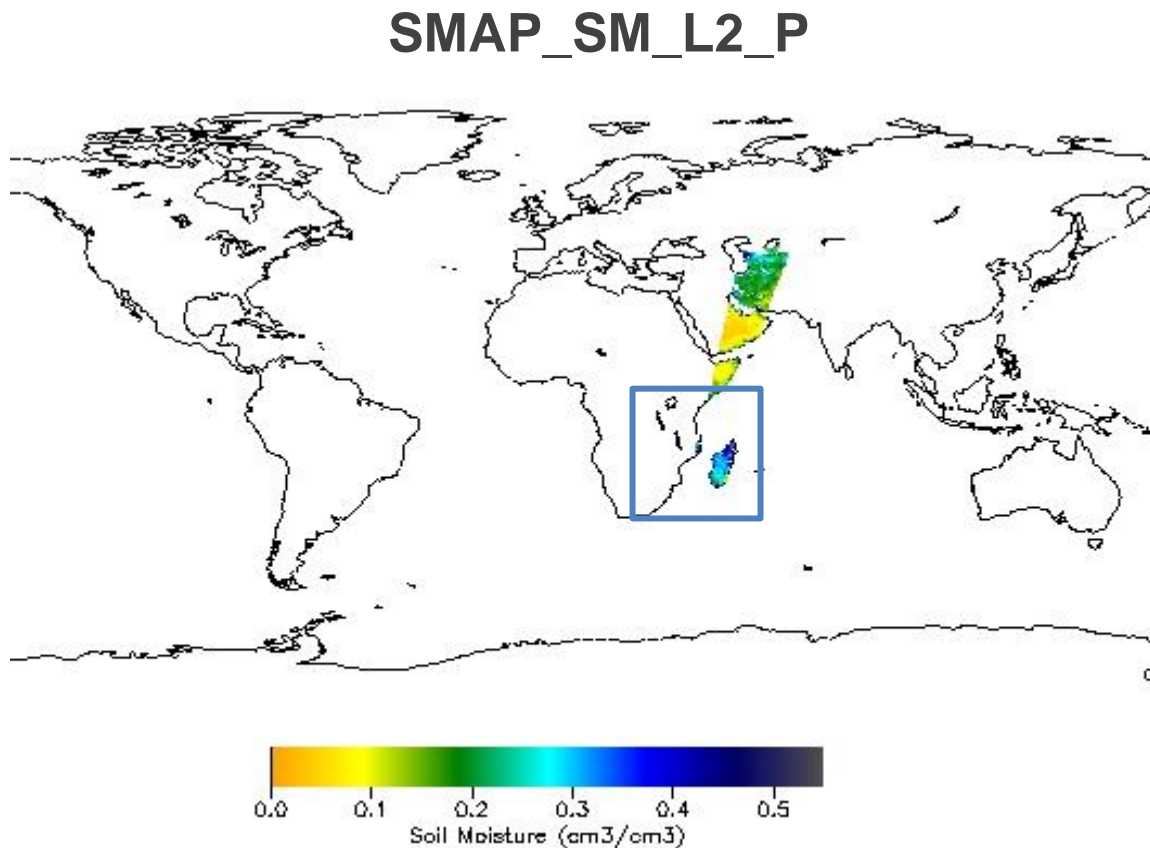
- Soil degradation: soil erosion, salinity are the main issues.
- Soil sealing (urbanization) of the already limited arable soils.
- Need to sustainable increase food production. Need of healthy soils.

Other soil parameters maps



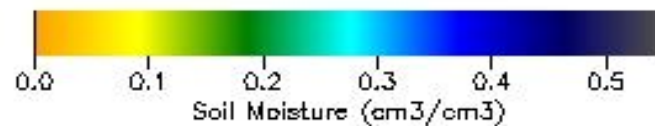
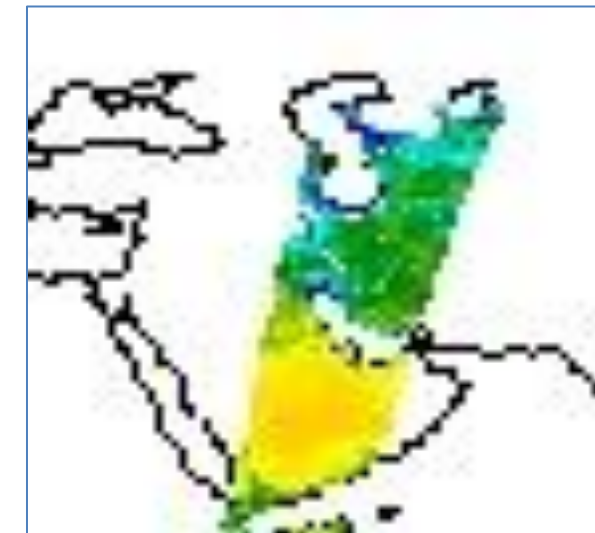
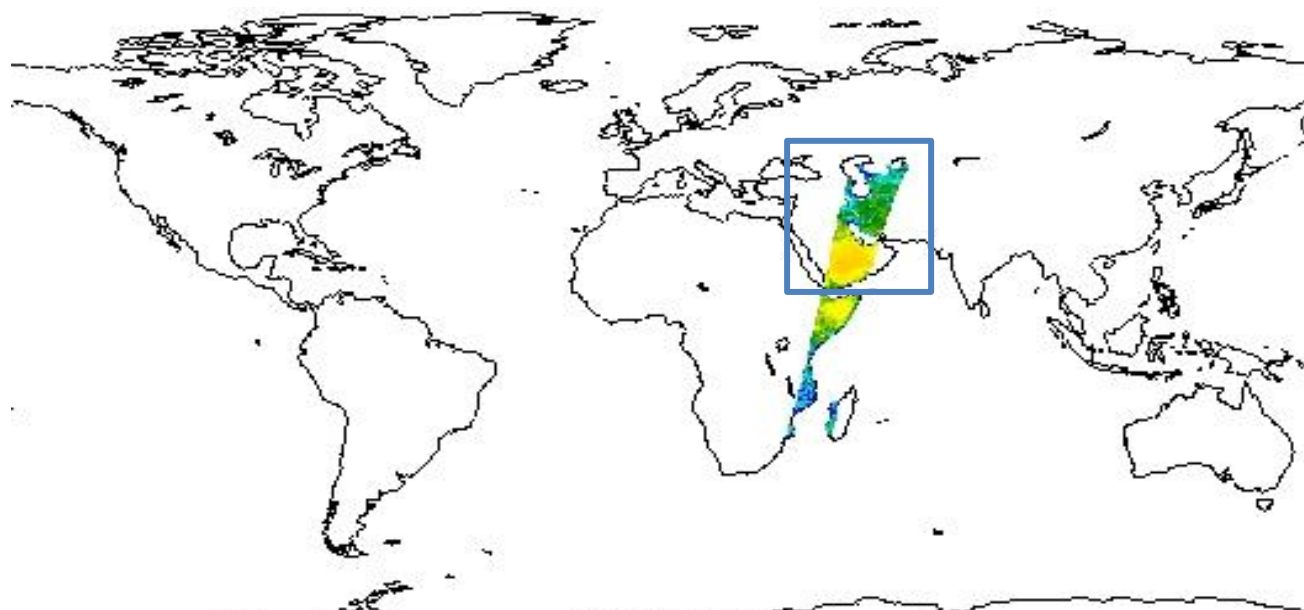
Gherboudj et al., 2016

Date: 2003 January 07, at 02:24 (UTC)



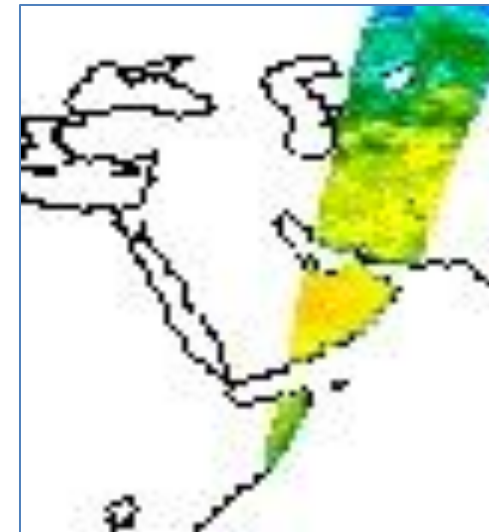
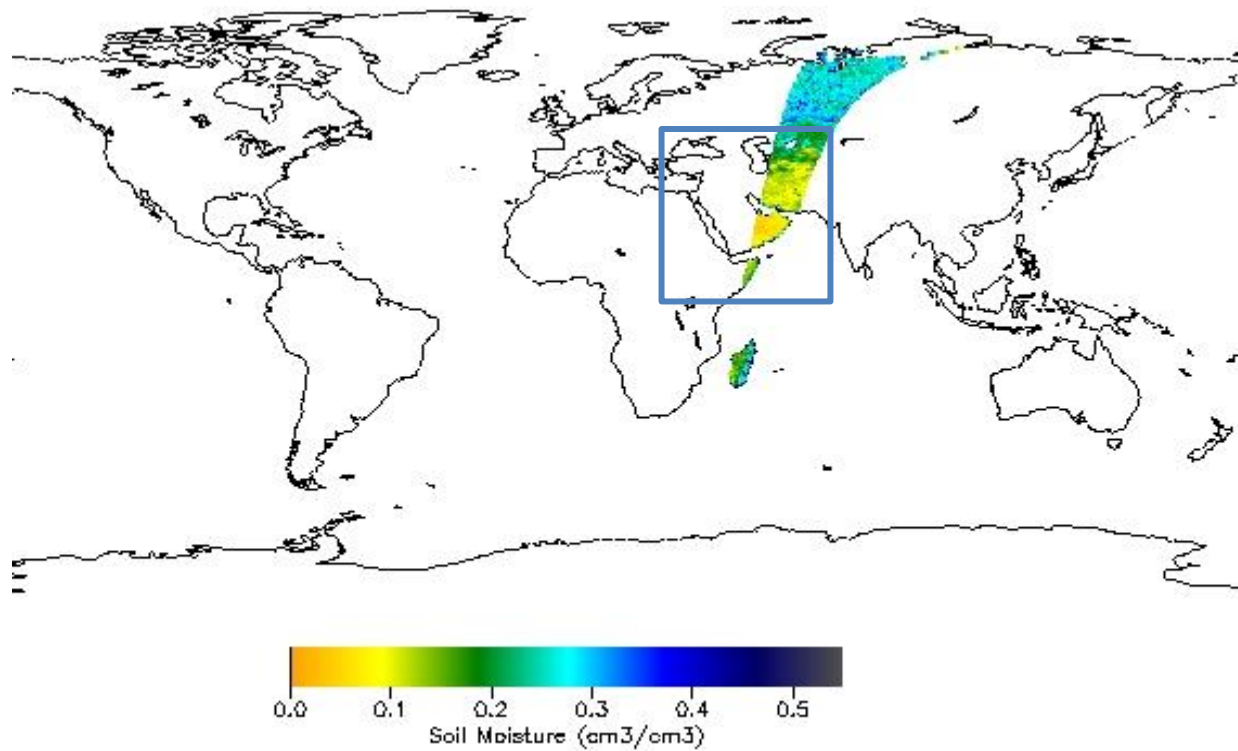
Date: 2003 January 10, at 02:36 (UTC)

SMAP_SM_L2_P

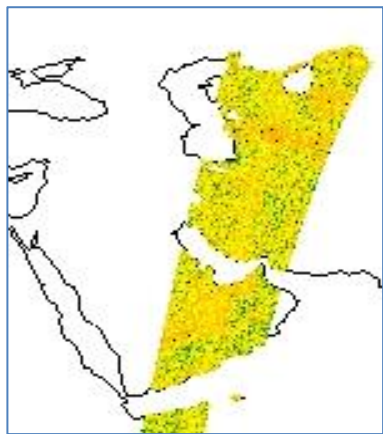


Date: 2003 June 13, at 02:12 (UTC)

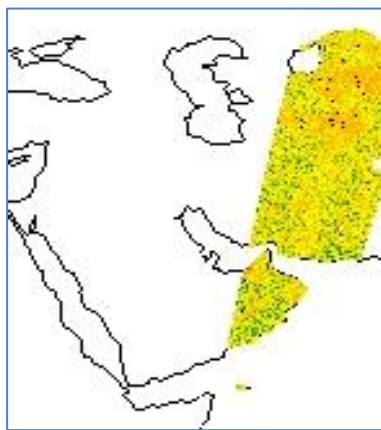
SMAP_SM_L2_P



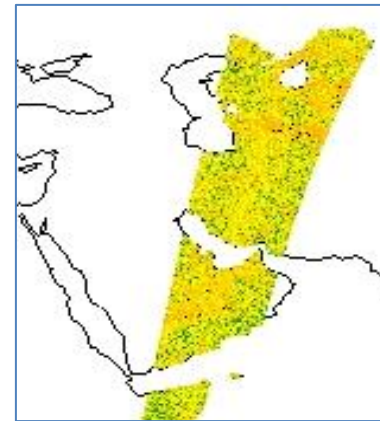
Level 2 Active Soil Moisture (SMAP_SM_L2_A)



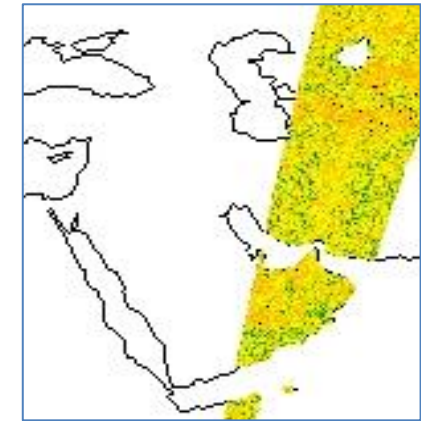
2003 March 28, at 02:24



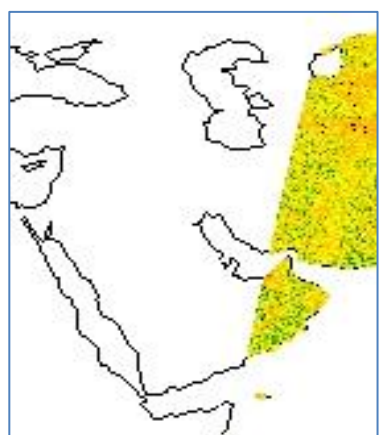
2003 March 30, at 00:00



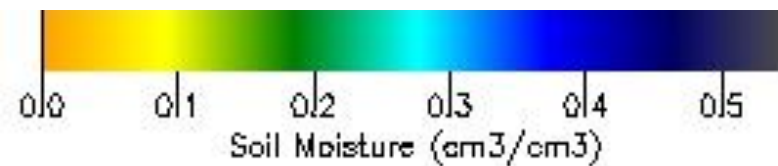
2003 April 05, at 02:24



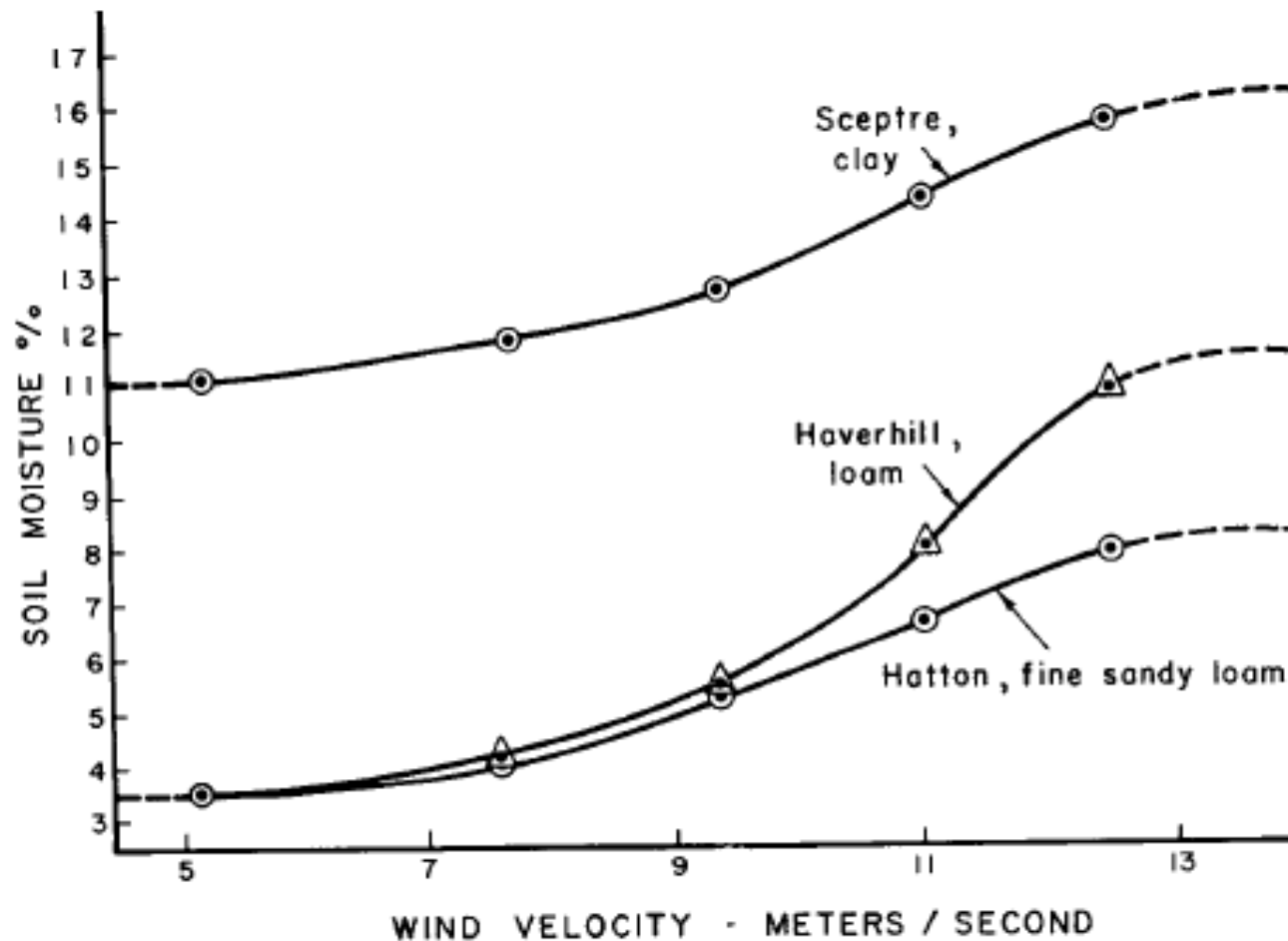
2003 May 04, at 02:12



2003 March, 20 at 02:24

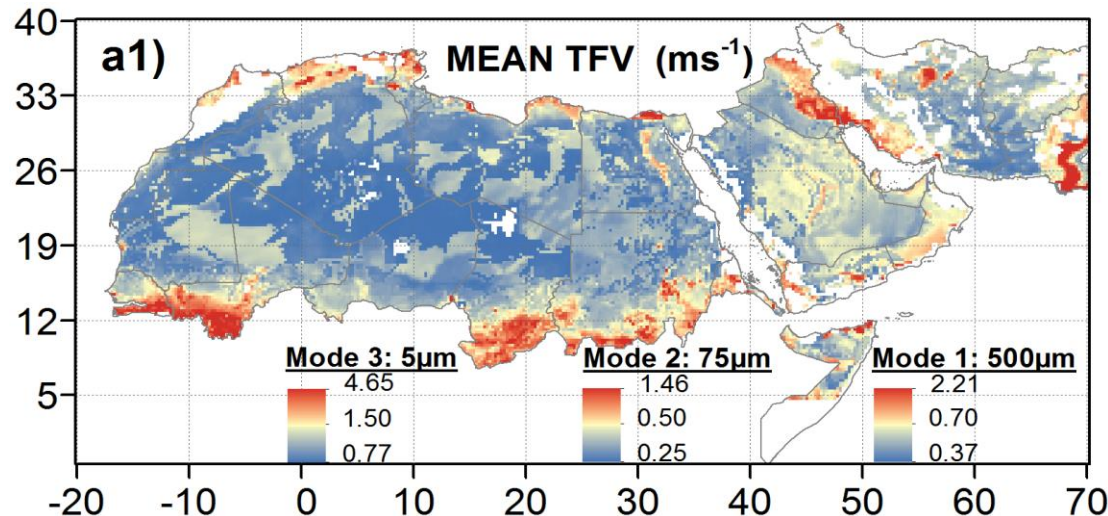


Soil Moisture versus friction velocity

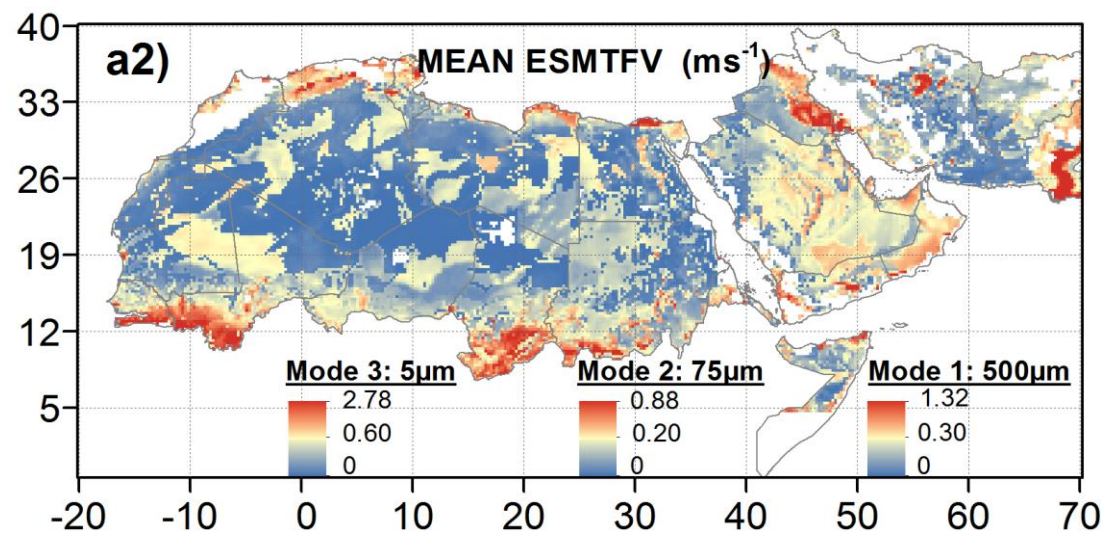


Threshold friction velocity increases with an increase in soil moisture

Effect of the soil moisture on the threshold friction velocity



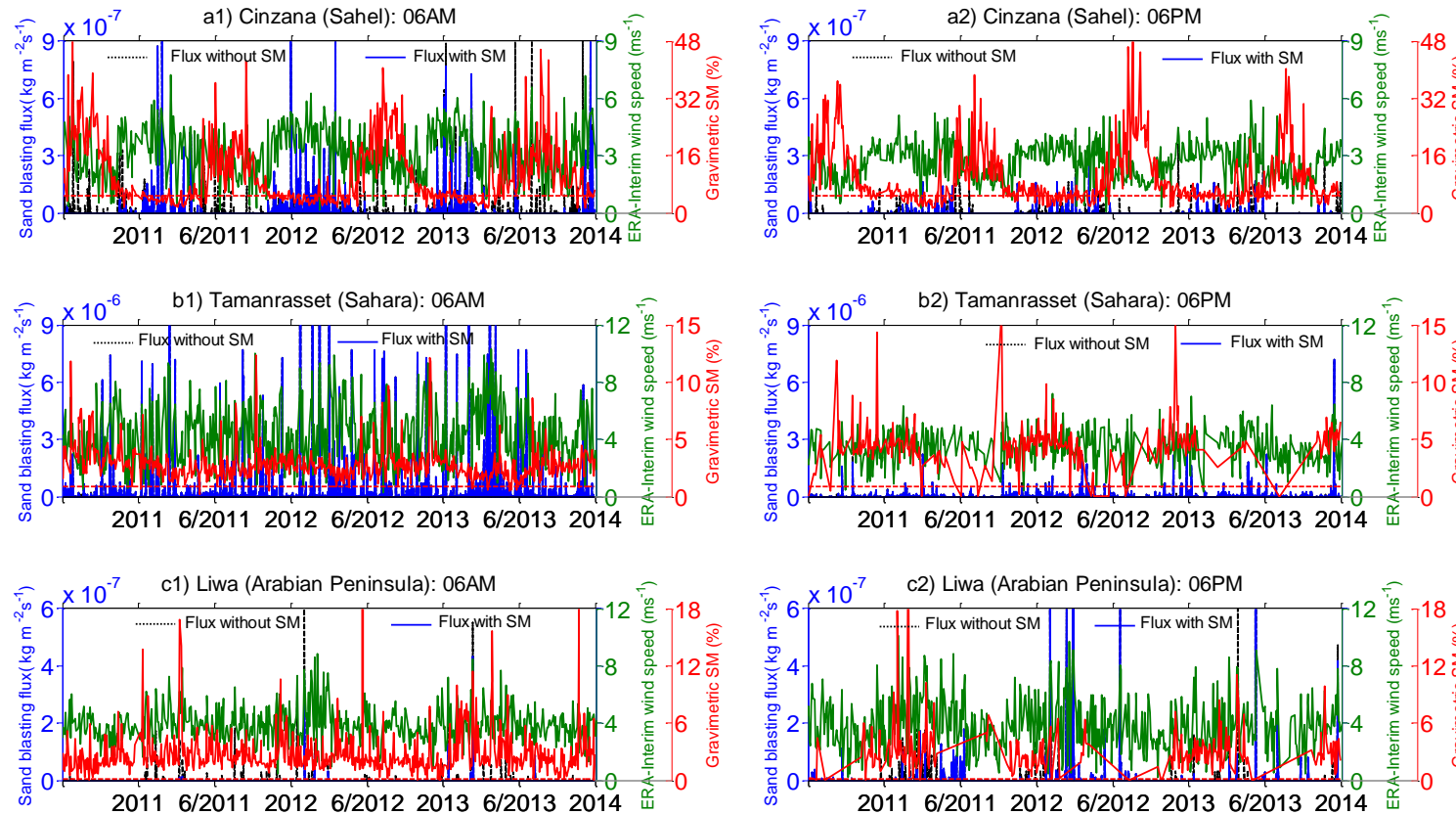
- Mean threshold friction velocity (TFV) over the MENA region has high spatial variability, which is found to correlate with the high soil moisture variability,
- Spatial pattern of the TFV is high over the Arabian Peninsula and low over the North-Africa.



- Spatial and temporal variability of the effect of the soil moisture on the TFV (ESMTFV, ms^{-1}) is high over the semi-arid area (mean and STD values reach 0.85ms^{-1} and 0.30ms^{-1} at particle size of 75 μm) and low over the arid area (higher temporal variability are associated with the sudden sporadic showers characterizing the desert climate)

Gherboudj et al., 2016

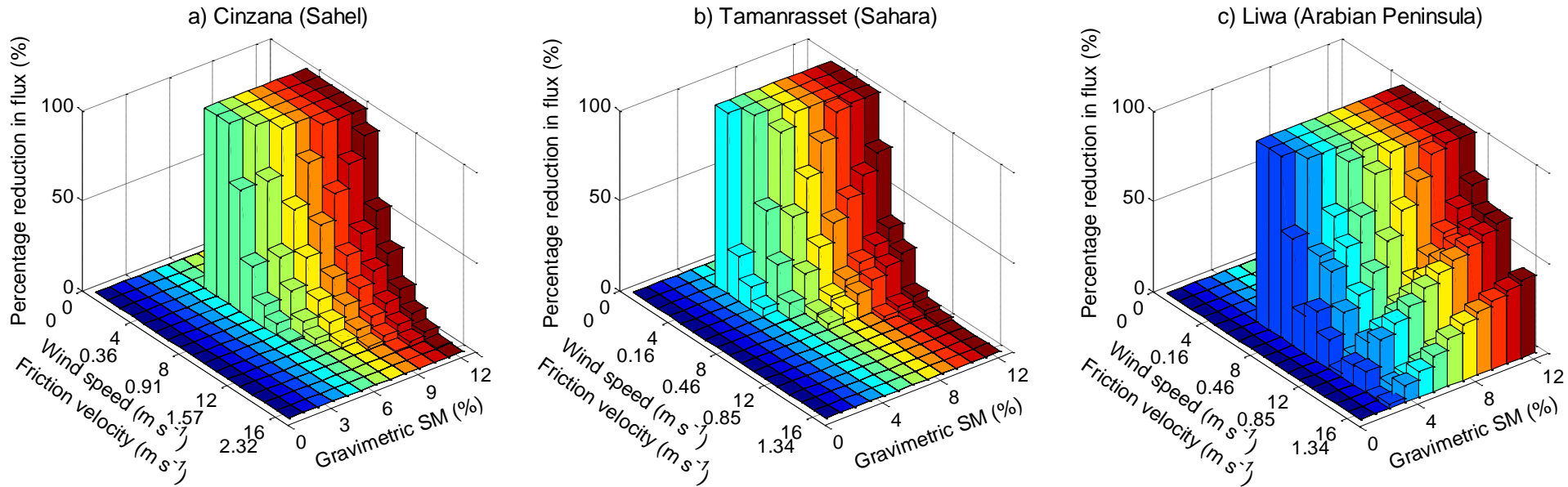
Time series of dust emission flux



Gravimetric soil moisture and sandblasting flux are inversely dependent, i.e. an increase in the gravimetric soil moisture causes a decrease in the sandblasting flux.

Gherboudj et al., 2016

Sensitivity analysis of the dust flux to the friction velocity and gravimetric soil moisture



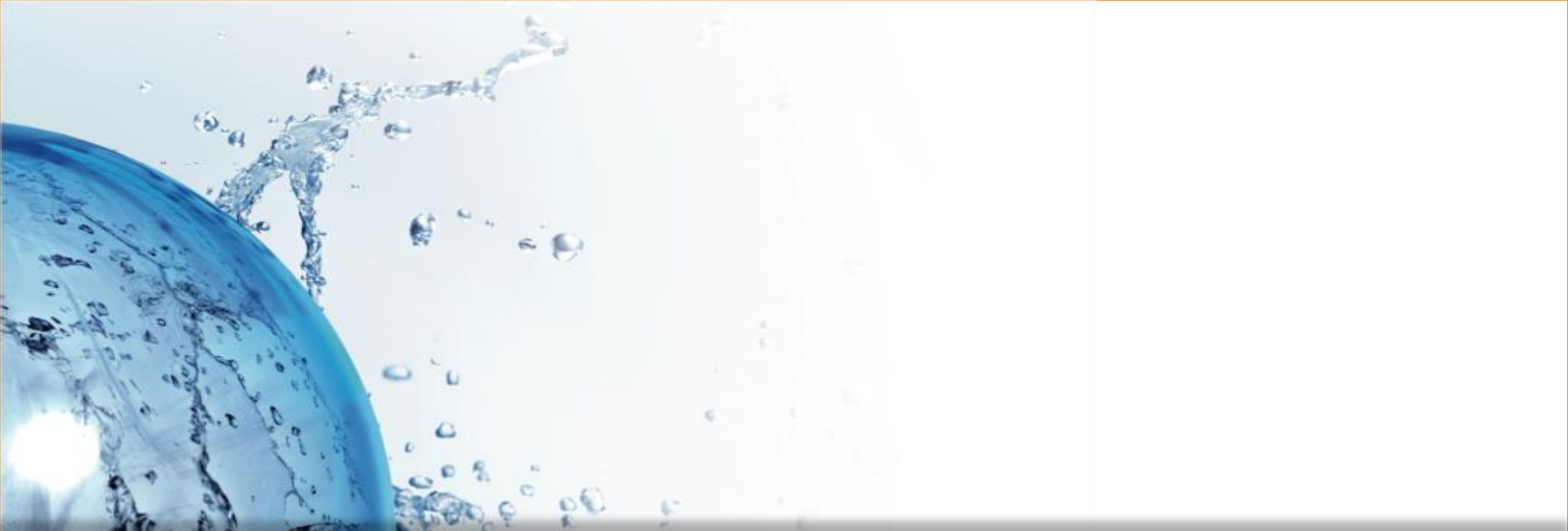
- No reduction in flux is observed for low friction velocity for all the considered soil moisture values.
- Significant reduction in the flux is observed when the soil moisture exceeded its threshold and the wind speed was greater than the threshold friction velocity
- At any given friction velocity value, the percentage reduction of the sandblasting flux increased as the soil moisture increased. However, this dependence is dominant at low friction velocity, close to the TTV (~100%), and low at high friction velocity (~30%),

Project Milestones

- 🌀 Import and adapt existing decision-support tools for dust retrieval. WMO SDS WS (Dust Retrieval from SEVIRI Images) and the US Air Force Weather Dust Transport Model.
- 🌀 Use SMAP Algorithm Testbed to generate high resolution soil moisture fields coincident with the several dust events occurred between 2003 and 2010.
- 🌀 Develop algorithm for soil moisture impact on dust generation using SMAP data attributes.
- 🌀 Assess impact of boundary layer growth and buoyancy on dust generation and vertical transport
- 🌀 Gridding and analyzing meteorological (wind speed/direction; precipitation; visibility; humidity) and land cover data.
- 🌀 Develop statistical experiment design to quantitatively assess the impact of SMAP data in the new dust generation and transport decision support model
- 🌀 Producing erosion threshold velocity ratios for different land covers (sand types)

Project Metrics

- ⌚ Two quantitative metrics were identified to assess the impact of SMAP products on dust generation estimation:
 - ⌚ The cross-sectional correlation (or time series correlation)
 - ⌚ The root mean square error (RMSE)
- The use of a higher spatial resolution of SMAP-derived SM is expected to improve the accuracy of estimating dust emissions since our dust maps have already a resolution of 4 km.



THANK YOU

